Extreme sea level implications of 1.5 °C, 2.0 °C, and 2.5 °C temperature stabilization targets in the 21st and 22nd centuries

Environmental Research Letters

LETTER

Extreme sea level implications of 1.5 °C, 2.0 °C, and 2.5 °C temperature stabilization targets in the 21st and 22nd centuries

D J Rasmussen[1,7], Klaus Bittermann[2], Maya K Buchanan[1,6], Scott Kulp[3], Benjamin H Strauss[3], Robert E Kopp[5] and Michael Oppenheimer[1,4]

[1] Woodrow Wilson School of Public & International Affairs, Princeton University, Princeton, NJ, United States of America
[2] Department of Earth and Ocean Sciences, Tufts University, Medford, MA, USA and Potsdam Institute for Climate Impact Research, Potsdam, Germany
[3] Climate Central, Princeton, NJ, United States of America
[4] Department of Geosciences, Princeton University, Princeton, NJ, United States of America
[5] Department of Earth & Planetary Sciences and Institute of Earth, Ocean, & Atmospheric Sciences, Rutgers University, New Brunswick, NJ, United States of America
[6] ICF International (Climate Adaptation and Resilience), New York, NY, United States of America
[7] Author to whom any correspondence should be addressed.

E-mail: dj.rasmussen@princeton.edu

Keywords: sea level rise, coastal flooding, climate change impacts, paris agreement, IPCC, extreme sea levels

Supplementary material for this article is available online

OPEN ACCESS

RECEIVED
21 October 2017

REVISED
31 January 2018

ACCEPTED FOR PUBLICATION
2 February 2018

PUBLISHED
15 March 2018

Abstract

Sea-level rise (SLR) is magnifying the frequency and severity of extreme sea levels (ESLs) that can cause coastal flooding. The rate and amount of global mean sea-level (GMSL) rise is a function of the trajectory of global mean surface temperature (GMST). Therefore, temperature stabilization targets (e.g. 1.5 °C and 2.0 °C of warming above pre-industrial levels, as from the Paris Agreement) have important implications for coastal flood risk. Here, we assess, in a global network of tide gauges, the differences in the expected frequencies of ESLs between scenarios that stabilize GMST warming at 1.5 °C, 2.0 °C, and 2.5 °C above pre-industrial levels. We employ probabilistic, localized SLR projections and long-term hourly tide gauge records to estimate the expected frequencies of historical and future ESLs for the 21st and 22nd centuries. By 2100, under 1.5 °C, 2.0 °C, and 2.5 °C GMST stabilization, the median GMSL is projected to rise 48 cm (90% probability of 28–82 cm), 56 cm (28–96 cm), and 58 cm (37–93 cm), respectively. As an independent comparison, a semi-empirical sea level model calibrated to temperature and GMSL over the past two millennia estimates median GMSL rise within 7–8 cm of these projections. By 2150, relative to the 2.0 °C scenario and based on median sea level projections, GMST stabilization of 1.5 °C spares the inundation of lands currently home to about 5 million people, including 60 000 individuals currently residing in Small Island Developing States. We quantify projected changes to the expected frequency of historical 10-, 100-, and 500-year ESL events using frequency amplification factors that incorporate uncertainty in both local SLR and historical return periods of ESLs. By 2150, relative to a 2.0 °C scenario, the reduction in the frequency amplification of the historical 100 year ESL event arising from a 1.5 °C GMST stabilization is greatest in the eastern United States, with ESL event frequency amplification being reduced by about half at most tide gauges. In general, smaller reductions are projected for Small Island Developing States.

1. Introduction

Extreme sea levels (ESLs) are defined as the combined height of the astronomical tide and storm surge (i.e. the storm tide) and mean sea level. ESLs can cause coastal floods that threaten life and property when flood defenses are over-topped. Rising mean sea levels are already magnifying the frequency and severity of ESLs that lead to coastal floods (Buchanan *et al* 2017, Sweet and Park 2014) and, by the end of the

century, coastal flooding may be among the costliest impacts of climate change in some regions (Hsiang *et al* 2017, Diaz 2016, Hinkel *et al* 2014). Sea-level rise (SLR) is expected to permanently inundate low-lying geographic areas (Marzeion and Levermann 2014, Strauss *et al* 2015), but these locations will first experience decreases in the return periods of ESL events and associated coastal floods (e.g. Hunter 2012, Sweet and Park 2014).

The rate of global mean sea-level (GMSL) rise depends on the trajectory of global mean surface temperature (GMST; Rahmstorf 2007, Kopp *et al* 2016a, Vermeer and Rahmstorf 2009), with the long-term committed amount of GMSL largely determined by the stabilized level of GMST (Levermann *et al* 2013). Thus, the management of GMST has important implications for regulating future GMSLs (Schaeffer *et al* 2012), and consequently the frequency and severity of ESLs and coastal floods. However, GMST stabilization does not imply stabilization of all climate variables. Under stabilized GMST, GMSL is expected to continue to rise for centuries, due to the long residence time of anthropogenic CO_2, the thermal inertia of the ocean, and the slow response of large ice sheets to forcing (Clark *et al* 2016, Levermann *et al* 2013, Held *et al* 2010). For instance, Schaeffer *et al* (2012) found that a 2.0 °C GMST stabilization would lead to a GMSL rise (relative to 2000) of 0.8 m by 2100 and >2.5 m by 2300, but if the GMST increase were held below 1.5 °C, GMSL rise at the end of the 23rd century would be limited to ~1.5 m. These findings suggest that selection of climate policy goals could have critical long-term consequences for the impacts of future SLR and coastal floods (Clark *et al* 2016).

The Paris Agreement seeks to stabilize GMST by limiting warming to 'well below 2.0 °C above pre-industrial levels' and to further pursue efforts to 'limit the temperature increase to 1.5 °C above pre-industrial levels' (UNFCCC 2015a). However, a recent literature review under the United Nations Framework Convention on Climate Change (UNFCCC) found the notion that 'up to 2.0 °C of warming is considered safe, is inadequate' and that 'limiting global warming to below 1.5 °C would come with several advantages' (UNFCCC 2015b). The advantages and disadvantages of each GMST target as they relate to coastal floods and ESLs have not been quantified. This is critical, as >625 million people currently live in coastal zones with <10 m of elevation, and population growth is expected in these areas (Neumann *et al* 2015). Examining the short- and long-term ESL implications of 1.5 °C and 2.0 °C GMST stabilization scenarios, as others have recently done for other climate impacts (e.g. Schleussner *et al* 2016a, 2016b, Mitchell *et al* 2017, Mohammed *et al* 2017), may better inform the policy debate regarding the selection of GMST goals.

In this study, we employ probabilistic, localized SLR projections to assess differences in the frequency of ESLs across 1.5 °C, 2.0 °C, and 2.5 °C GMST stabilization scenarios at a global network of 194 tide gauges (section 2.1). We use long-term hourly tide gauge records and extreme value theory to estimate present and future return periods of ESL events (section 2.4.1). We extend our analysis through the 22nd century to account for continuing SLR in order to inform multi-century planning and infrastructure investments. Lastly, we assess differences in the exposure of current populations to future SLR under 1.5 °C, 2.0 °C, and 2.5 °C GMST stabilizations (section 3.2). Unlike deterministic or median estimates, the use of probabilistic projections allows for the characterization of uncertainty, which is important for risk management.

Various approaches have been used to project GMSL under GMST targets. For instance, Jevrejeva *et al* (2016) estimate future local SLR under a GMST increase of 2 °C using a representative concentration pathway (RCP) 8.5 GMST trajectory that passes through 2 °C of warming by mid-century, but this approach likely underestimates SLR relative to a scenario that achieves 2 °C GMST stabilization by 2100 as it neglects the time-lagged, integrated response of the ocean and cryosphere to warming (Clark *et al* 2016). More generally, studies that condition future ESL or flood projections on the RCPs may be insufficient for assessing the costs and benefits of climate policy scenarios, such as GMST stabilization targets (e.g. Section 13.7.2.2 of Church *et al* 2013, Buchanan *et al* 2017, Hunter 2012, Tebaldi *et al* 2012). The RCPs are designed to be representative of a range of emissions scenarios that result in prescribed anthropogenic radiative forcings by 2100 relative to pre-industrial conditions (e.g. 8.5 $W m^{-2}$ for RCP8.5). They are not representative of a specific emissions trajectory, climate policy (e.g. GMST target), or socioeconomic and technological change (Moss *et al* 2010, van Vuuren *et al* 2011). Recently, Jackson *et al* (2018) produced probabilistic, localized SLR projections under 1.5 °C and 2.0 °C GMST targets, but did not assess ESLs or consider sea-level change after 2100, the latter being necessary for evaluating the effects of GMST stabilization.

Semi-empirical sea level (SESL) models (Rahmstorf *et al* 2012) can estimate future GMSL rise under various GMST scenarios (e.g. Schaeffer *et al* 2012, Bittermann *et al* 2017). Unlike their process-based counterparts (e.g. Kopp *et al* 2014), SESL models do not explicitly model individual physical components of sea-level change. They are calibrated over a historical period using the observed statistical relationship between GMSL and a climate parameter (such as GMST). Assuming these relationships hold in the future, SESL models project the rate of GMSL change conditional upon a GMST pathway (e.g. Rahmstorf 2007, Vermeer and Rahmstorf 2009, Kopp *et al* 2016a). However, SESL models do not produce estimates of local SLR, which are necessary for

local risk assessment and adaptation planning because local SLR can substantially differ from the global mean (Milne *et al* 2009).

2. Methods

We project probabilistic global and local sea level conditional on GMST stabilization at 1.5 °C, 2.0 °C, and 2.5 °C using the component-based, local sea level projection framework from Kopp *et al* (2014, henceforth K14). We compare the GMSL projections from the K14 framework to those from the SESL model of Kopp *et al* (2016a) and Bittermann *et al* (2017). While SESL models cannot produce local projections of SLR, they can serve as a reference point for evaluating the consistency of process-based projections with historical temperature-GMSL relationships. The flow and sources of information used to construct the local SLR and GMSL projections using the K14 method is depicted in figure S-1(*a*), while the flow of information used to generate the SESL projections is provided in figure S-1(*b*). Local SLR projections from the K14 approach are combined with historical distributions of ESL events to estimate future return periods of historical ESL events (figure S-1(*a*)), similar to the approaches by Buchanan *et al* (2017, 2016) and Wahl *et al* (2017).

2.1. Component-based model approach: global and local sea-level rise projections

Sea-level change does not occur uniformly. Dynamic ocean processes (Levermann *et al* 2005), changes to temperature and salinity (i.e. steric processes), and changes in the Earth's rotation and gravitational field associated with water-mass redistribution (e.g. land-ice melt; Mitrovica *et al* 2011), as well as glacial isostatic adjustment (GIA; Farrell and Clark 1976) and other drivers of vertical land motion cause local relative sea levels to differ from the global mean. We model local relative sea level using the K14 framework, but make modifications to accommodate the stratification of atmosphere–ocean general circulation models (AOGCMs) and RCPs into groups that meet GMST stabilization targets (see section 2.2). AOGCM output from the Coupled Model Intercomparison Project (CMIP) Phase 5 archive (Taylor *et al* 2012) forced with the RCPs (to 2100) and their extensions (to 2300) are used directly for global mean thermal expansion (TE) and local ocean dynamics, and as a driver of a surface mass balance (SMB) model of glaciers and ice caps (GICs; Marzeion *et al* 2012). Antarctic ice sheet (AIS) and the Greenland ice sheet (GIS) contributions are estimated using a combination of the Intergovernmental Panel on Climate Change's (IPCC) Fifth Assessment Report (AR5) projections of ice sheet dynamics and SMB (table 13.5 in Church *et al* 2013) and expert elicitation of total ice sheet mass loss from Bamber and Aspinall (2013). As in AR5, ice sheet SMB contributions are represented as being dependent on the forcing scenario, while ice sheet dynamics are not. A spatiotemporal Gaussian process regression model is used with tide gauge data to estimate the long-term contribution from non-climatic factors such as tectonics, GIA, delta processes (e.g. sediment compaction), and human-induced subsidence. Changes in the rate of human-induced subsidence are not considered. Global mean land water storage effects are modeled using relationships between population and groundwater removal and impoundment (Kopp *et al* 2014). To generate probability distributions of global and local mean sea level for each GMST scenario at tide gauges (table S-1), we use 10 000 Latin hypercube samples of probability distributions of individual sea level component contributions.

2.2. Approximating global temperature stabilization with RCPs

The RCP-driven experiments in the CMIP5 archive are not designed to inform the assessment of climate impacts from incremental temperature changes. As such, we construct alternative ensembles for 1.5 °C, 2.0 °C, and 2.5 °C scenarios using CMIP5 output filtered according to each AOGCM's 2100 GMST. Specifically, we create ensembles for 1.5 °C, 2.0 °C, and 2.5 °C scenarios with AOGCMs that have a 21st century GMST increase (19 year running average) of 1.5 °C, 2.0 °C, and 2.5 °C (±0.25 °C). For consistency with the K14 framework, which models 19 year running averages of SLR relative to 2000, GMST is anomalized to 1991–2009 and then shifted upward by 0.72 °C to account for warming since 1875–1900 (Hansen *et al* 2010, GISSTEMP Team 2017). Selection of the AOGCMs for each scenario ensemble is made irrespective of the AOGCM's RCP forcing. For model outputs that end in 2100, we extrapolate the 19 year running average GMST to 2100 based on the 2070–2090 trend. While we chose 2100 as the determining year for which AOGCMs are selected for each ensemble, it should be noted that Article 2 of the UNFCCC (UNFCCC 1992) does not require that GMST stabilization be achieved within a particular timeframe. The Paris Agreement likewise does not specify a timeframe for GMST stabilization, though its goal of bringing net greenhouse gas (GHG) emissions to zero in the second half of the 21st century implies a similar timeframe for stabilization. We make the assumption that AOGCM outputs that end at 2100 either stay within the range of the target ±0.25 °C or fall below by any amount (i.e. undershoot). For AOGCMs that have GMST output available after 2100, only those that undershoot the target are retained. However, we make an exception to this rule for the 2.5 °C scenario ensemble in order to include AOGCMs for generating post-2100 projections. For RCP4.5 and RCP6, GMST stabilization should not occur before 2150, when GHG concentrations stabilize (Meinshausen *et al* 2011b) and so SLR projections after 2100 may

not be representative of conditions under true GMST stabilization. The GMST trajectories and GMSL contributions from TE and glacial ice from selected CMIP5 models that are binned into 1.5 °C, 2.0 °C, and 2.5 °C GMST categories are shown in figures 1 and S-2, respectively. Table S-2 lists the AOGCMs employed in each GMST scenario ensemble and the sea-level components used. Given the paucity of CMIP5 output after 2100, the range of TE and GIC contributions to SLR in the 22nd century is likely underestimated relative to the 21st century. Total ice sheet contributions from AR5 are calculated for each GMST scenario by randomly sampling AIS and GIS ice sheet distribution for each RCP (table 13.5 in Church *et al* 2013) in proportion to the representation of each RCP in the groups of CMIP5 models selected for each GMST scenario[8].

2.3. GMSL rise projections from a SESL model

We generate estimates for GMSL for 2000–2200 using the SESL model from Kopp *et al* (2016a) and Bittermann *et al* (2017) driven with both GMST trajectories from CMIP5 models (figure 1) and GMST trajectories from the reduced-complexity climate model MAGICC6 (Meinshausen *et al* 2011a, as employed in Rasmussen *et al* 2016) for 2100 GMST targets of 1.5 °C, 2.0 °C, and 2.5 °C (±0.25 °C) (figure S-3). The MAGICC6 GMST trajectories are selected from all RCP-grouped projections using the same criteria as in section 2.2. The SESL model is calibrated to the common era temperature reconstruction from Mann *et al* (2009) and the sea level reconstruction of Kopp *et al* (2016a). The historical statistical relationship between temperature and the rate of sea-level change is assumed to be constant; not included are nonlinear physical processes or critical threshold events that could substantially contribute to SLR, such as ice sheet collapse (Kopp *et al* 2016b, Levermann *et al* 2013). Threshold behavior is partially incorporated in the K14 framework through expert assessments of future ice sheet melt contributions (Bamber and Aspinall 2013), which may be one reason why the K14 framework produces higher estimates in the upper tail of the SLR probability distribution.

2.4. Estimating the frequency of historical and future extreme sea level events

The heights of historical ESL events that result from tropical and extra-tropical cyclones, extreme astronomical tides, and other processes are recorded in sub-daily tide gauge observations. Extreme value theory can be used with these tide gauge measurements to estimate the historical return levels of ESL events, including events that occur less often, on average, than the length of the observational record. For example, one could use extreme value theory to estimate the height of the present-day 500 year (or 0.2% average annual probability) ESL event from a record that is <500 years in length. Assuming no non-linear relationships between SLR and ESL events and no change in the frequency and intensity of processes that cause ESLs (e.g. tropical and extra-tropical cyclones), the estimated return levels of historical ESL events can be combined with local SLR projections to estimate the return levels of future ESL events.

2.4.1. Estimation of historical return levels of extreme sea levels

Here, we use extreme value theory with daily maximum sea levels at tide gauges archived by the University of Hawaii Sea Level Center (see supplementary data; Caldwell *et al* 2015) to estimate historical return levels of ESL events. Specifically, we follow Tebaldi *et al* (2012) and Buchanan *et al* (2016, 2017) and employ a generalized Pareto distribution (GPD) and a peaks-over-threshold approach (Coles 2001b, 2001a). The GPD describes the probability of a given ESL height conditional on an exceedance of the GPD threshold. We use the 99th percentile of daily maximum sea levels as the GPD threshold, which is generally both above the highest seasonal tide and balances the bias-variance trade-off in the GPD parameter estimation (Tebaldi *et al* 2012). The number of annual exceedances of the GPD threshold is assumed to be Poisson distributed with mean λ. Tide gauge observations are detrended and referenced to mean higher high water (MHHW)[9] and the GPD parameters are estimated using the method of maximum likelihood (see supplementary data). Uncertainty in the GPD parameters is calculated from their estimated covariance matrix and is sampled using Latin hypercube sampling of 1000 normally distributed GPD parameter pairs. For a given tide gauge, the annual expected number of exceedances of ESL height z is given by $N(z)$:

$$N(z) = \begin{cases} \lambda\left(1 + \frac{\xi(z-\mu)}{\sigma}\right)^{-\frac{1}{\xi}} & \text{for} \quad \xi \neq 0 \\ \lambda \exp\left(-\frac{z-\mu}{\sigma}\right) & \text{for} \quad \xi = 0 \end{cases} \quad (1)$$

where the shape parameter (ξ) governs the curvature and upward statistical limit of the ESL event return curve, the scale parameter (σ) characterizes the variability in the exceedances caused by the combination of tides and storm surges, and the location parameter (μ) is the threshold water-level above which return levels are estimated with the GPD, here the 99th percentile of daily maximum sea levels. Meteorological and hydrodynamic differences between sites give rise

[8] For example, the 1.5 °C GMST employs 12 CMIP5 models from RCP2.6 and 2 from RCP4.5, so 86% of the samples aredrawn from the RCP2.6 distribution and 14% are drawn from the RCP4.5 distribution (supplementary information (SI), table S-2 available at stacks.iop.org/ERL/13/034040/mmedia).

[9] Here defined as the average level of high tide over the last 19-years in each tide gauge record, which is different from the current US National Tidal Datum Epoch of 1983–2001.

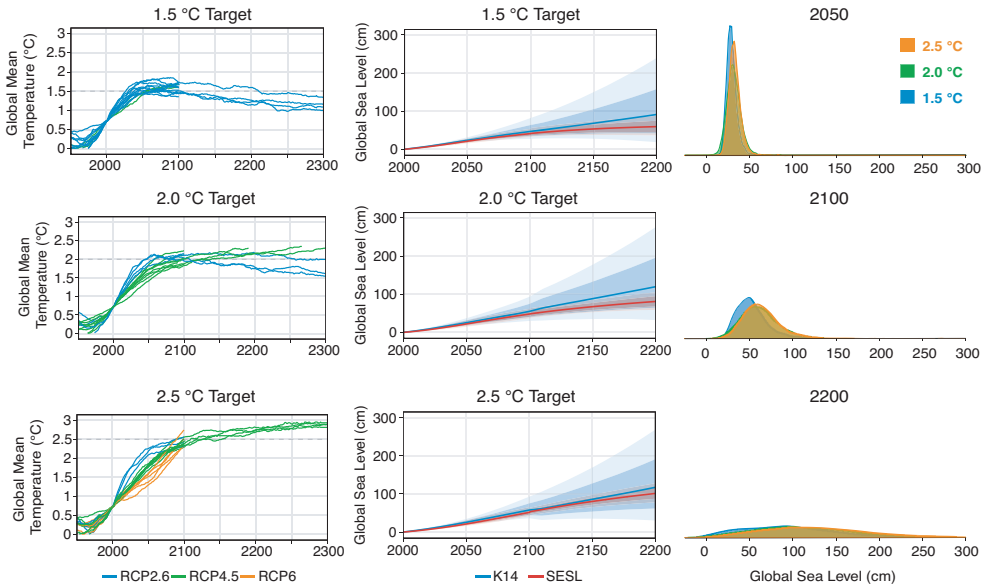

Figure 1. Left column: GMST trajectories from CMIP5 models (1950–2300) that have a 19 year running average 2100 GMST of 1.5 °C, 2.0 °C, and 2.5 °C ±0.25 °C (relative to 1875–1900; blue = RCP2.6, green = RCP4.5, orange = RCP6). GMST is anomalized to 1991–2009 and shifted up by 0.72 °C to account for warming since 1875–1900 (Hansen *et al* 2010, GISSTEMP Team 2017). Table S-2 (SI) lists the CMIP5 models used for each GMST target. Middle column: GMSL rise (cm; relative to 2000) from the methodology of Kopp *et al* (2014) (K14; blue), using CMIP5 temperature trajectories from the left column, and a SESL model from Kopp *et al* (2016a) (red). Temperature trajectories that drive the SESL model are shown in the left column. The thick line is the 50th percentile, heavy shading is the 17/83rd percentile, and light shading is the 5/95th percentile. Right column: probability distributions of projected 2050, 2100, and 2200 global mean sea-level rise for GMST stabilization targets using the Kopp *et al* (2014) framework (blue = 1.5 °C, green = 2.0 °C, orange = 2.5 °C).

to differences in the shape parameter (ξ). ESL frequency distributions with $\xi > 0$ are 'heavy tailed', due to a higher frequency of events with extreme high water (e.g. tropical and extra-tropical cyclones). Distributions with $\xi < 0$ are 'thin tailed' and have a statistical upper bound on extreme high water levels. Events that occur between λ and 182.6/year (i.e. exceeding MHHW half of the days per year) are modeled with a Gumbel distribution, as they are outside of the support of the GPD. Note that ESL events at tide gauges are not referred to as floods as the occurrence of an actual flood depends on the level of coastal flood protection, terrain, infrastructure, and other local factors.

2.4.2. *Extreme sea level event frequency amplification factors*

The frequency amplification factor (AF) quantifies the increase in the expected frequency of historical ESL events (e.g. the 100 year ESL event) due to SLR (Buchanan *et al* 2017, Hunter 2012, Church *et al* 2013). Due to variation in the local storm climate and hydrodynamics, the height of ESL event return levels are unique to each location (SI, figure S-4). The calculation of the expected AF includes both the uncertainty in the estimates of the return periods of historical ESL events and uncertainty in SLR projections. Following Buchanan *et al* (2017), we define the expected ESL event frequency amplification factor AF(z) for ESL events with height z as the ratio of the expected number of ESL events after including uncertain SLR to the historical expected number of ESL events:

$$\mathrm{AF}(z) = \frac{E[N(z-\delta)]}{N(z)} \qquad (2)$$

where $N(z–\delta)$ is the annual expected number of exceedances of ESL height z after including SLR (δ), $E[\cdot]$ is the expectation operator applied to the full probability distribution of SLR projections, and $N(z)$ is the historical annual expected number of exceedances of ESL height z.

2.4.3. *Assessment of population exposure*

Following the methods used in Kopp *et al* (2017), we assess the current population living on land exposed to future permanent inundation from GMSL under each GMST stabilization scenario. We emphasize that this is not a literal measure of future population exposure—which will depend upon population growth, the dynamic response of the population to rising sea levels, and coastal protective measures taken—but is instead intended to index the relevance of SLR to current economic development and cultural heritage under different GMST stabilizations. We use a 1 arc-sec SRTM 3.0 digital elevation model from NASA (NASA JPL 2013) referenced to local MHHW levels for the year 2000 and this study's local SLR projection grids. Projected inundation areas are intersected with

Table 1. GMSL projections. All values are cm above 2000 CE baseline. AIS = Antarctic ice sheet, GIS = Greenland ice sheet; TE = thermal expansion; GIC = glaciers and ice caps; LWS = land water storage. AIS and GIS ice sheet distributions for each RCP from the Intergovernmental Panel on Climate Change's Fifth Assessment Report (Church *et al* 2013) are randomly sampled in proportion to the RCP representation in the CMIP5 model filtering (table S-2). K16: SESL model from Kopp *et al* (2016a) driven with GMST trajectories from MAGICC (see SI figure S-3) and CMIP5 GMST trajectories (see figure 1); J18: Jackson *et al* (2018), S16: Schleussner *et al* (2016a).

	1.5 °C			2.0 °C			2.5 °C		
cm	50	17–83	5–95	50	17–83	5–95	50	17–83	5–95
2100—Components									
AIS	6	−4–17	−8–35	6	−5–17	−8–34	6	−5–16	−8–34
GIS	7	4–12	3–19	8	4–14	2–22	8	4–15	2–22
TE	19	14–23	10–27	25	15–34	7–42	26	20–31	16–35
GIC	11	8–13	6–15	11	7–16	2–21	13	11–15	9–17
LWS	5	3–7	2–8	5	3–7	2–8	5	3–7	2–8
Total	48	35–64	28–82	56	39–76	28–96	58	45–75	37–93
Projections by year									
2050	24	20–28	18–32	25	20–32	15–37	26	22–30	19–34
2070	34	27–41	24–50	38	28–48	21–58	38	32–47	27–55
2100	48	35–64	28–82	56	39–76	28–96	58	45–75	37–93
2150	69	42–107	28–151	88	50–133	25–181	86	54–126	35–171
2200	93	43–161	20–241	120	57–197	20–281	118	62–189	31–268
Other projections for 2100									
K16[a]	38	33–43	30–47	45	39–52	35–58	54	47–62	42–68
K16[b]	41	36–48	32–53	48	41–56	36–62	51	45–59	41–65
J18	44	30–58	20–67	50	35–64	24–74	–	–	–
S16	41	29–53	–	50	36–65	–	–	–	–
Other projections for 2200									
K16[a]	58	45–72	36–81	79	65–93	56–104	100	85–115	75–127
K16[b]	59	45–75	37–88	81	68–95	59–105	101	87–116	78–128

[a] SESL model driven with MAGICC6 GMST trajectories shown in SI figure S-3.

[b] SESL model driven with CMIP5 GMST trajectories shown in figure 1.

LandScan 2010 global population data on a 1 km × 1 km global grid (Bright *et al* 2011) and national boundary data (Hijmans *et al* 2012). For each GMST target, the current population on land at risk is assessed at the 5th, 50th, and 95th percentile local SLR projection. Further details are provided in the supplementary information of Kopp *et al* (2017).

3. Results

3.1. GMSL rise

The GMSL projections for each GMST target from the K14 and SESL method are shown in figure 1 and are tabulated along with the component contributions in table 1. For the K14 method, differences in median GMSL between 1.5 °C, 2.0 °C, and 2.5 °C GMST stabilization targets do not appear until after 2050, when the 1.5 °C scenario begins to separate from the 2.0 °C and 2.5 °C trajectories (table 1). The median GMST trajectories diverge earlier, around 2030 (figure S-3). This is consistent with the early to mid-century divergence in the radiative forcing pathways and this study's allocation of RCPs in the 1.5 °C (primarily RCP2.6), 2.0 °C (primarily RCP4.5), and 2.5 °C (primarily RCP4.5 and RCP6) scenarios (SI, table S-2). Median projections for 2100 GMSL under a 1.5 °C scenario are 48 cm, with a *very likely* range (90% probability) of 28–82 cm. An additional 8–10 cm of median GMSL rise is found for the 2.0 °C and 2.5 °C GMST scenarios, 56 cm (*very likely* 28–96 cm) and 58 cm (*very likely* 37–93 cm), respectively. Prior to mid-century, TE and GIC contributions account for more than half of GMSL projection uncertainty, but by 2100, ice sheet contributions dominate (SI, figure S-5). Other studies found similar GMSL results. Using the same framework, Kopp *et al* (2014) estimated median 2100 GMSL projections under RCP2.6 and RCP4.5 of 50 cm (*very likely* 29–82 cm) and 59 cm (*very likely* 36–93 cm), respectively. Jackson *et al* (2018) also employs the CMIP5 ensemble to estimate probabilistic local SLR projections for GMST stabilizations, but do not consider non-linear ice dynamics (e.g. Bamber and Aspinall 2013). Their median projections for 1.5 °C (44 cm; *very likely* 20–67 cm) and 2.0 °C (50 cm; *very likely* 24–74 cm) GMST stabilizations are within 4–6 cm of this study. Using a method that scales SLR component contributions as a function of GMST and ocean heat uptake (Perrette *et al* 2013), Schleussner *et al* (2016a) estimated a median 2100 GMSL for 1.5 °C and 2.0 °C scenarios, that is 6–7 cm lower than this study's K14 framework projections. (table 1).

Despite being warmer by a half-degree, the 2.5 °C GMSL projections largely overlap the 2.0 °C scenario (figure 1). Variation in the transient climate response and ocean heat uptake efficiency across CMIP5 models leads to weak correlation between TE and GMST ($r^2 = 0.10$; figure S-6; Kuhlbrodt and Gregory 2012, Raper *et al* 2002). As such, cooler models may produce more TE than warmer models, and vice versa. Ice sheet contributions are also similar between 2.0 °C and 2.5 °C scenarios (table 1). To test the sensitivity of model-RCP filtering to the choice of GMST stabilization, we additionally calculate GMSL under a 1.75 °C

Table 2. The current population (in millions) living on lands exposed to future permanent inundation from median (5th–95th percentile) local sea-level rise (SLR) projections. Population estimates are from 2010. The top five countries with the most exposure in 2150 are included in the table as well as United Nations defined SIDS.

Human population exposure under 2100 local SLR projections (millions)				
Region	Total Population	1.5 °C	2.0 °C	2.5 °C
World	6,836.42	46.12 (31.92–69.23)	48.76 (32.01–79.65)	50.35 (33.33–77.38)
China	1,330.20	11.70 (5.89–20.37)	12.75 (6.00–22.05)	13.26 (6.18–22.91)
Vietnam	89.55	6.57 (4.56–9.91)	6.96 (4.58–10.65)	7.16 (4.66–11.05)
Japan	126.66	4.44 (3.84–5.56)	4.62 (3.88–5.85)	4.69 (3.89–6.11)
Netherlands	16.78	4.71 (4.20–5.57)	4.86 (4.16–5.87)	4.85 (4.36–5.63)
Bangladesh	156.13	2.83 (1.98–4.33)	3.03 (2.05–4.77)	3.09 (2.13–4.92)
SIDS	62.08	0.40 (0.30–0.56)	0.42 (0.30–0.64)	0.43 (0.32–0.63)
Human population exposure under 2150 local SLR projections (millions)				
Region	Total Pop.	1.5 °C	2.0 °C	2.5 °C
World	6,836.42	56.05 (32.54–112.97)	61.84 (32.89–138.63)	62.27 (34.08–126.95)
China	1,330.20	14.46 (5.73–31.00)	16.92 (5.86–37.08)	16.58 (5.75–36.48)
Vietnam	89.55	7.60 (4.46–15.19)	8.47 (4.51–17.13)	8.33 (4.54–16.58)
Japan	126.66	4.92 (3.87–7.69)	5.40 (3.94–8.72)	5.35 (3.89–8.61)
Netherlands	16.78	5.06 (4.12–6.49)	5.18 (4.22–6.45)	5.28 (4.38–6.48)
Bangladesh	156.13	4.48 (2.58–9.78)	5.10 (2.67–11.95)	5.01 (2.82–11.15)
SIDS	62.08	0.46 (0.29–0.91)	0.52 (0.29–1.14)	0.52 (0.31–1.01)

and 2.25 °C GMST scenario. The median 2100 GMSL under the 1.75 °C scenario is 3 cm greater than the 1.5 °C scenario, and the 2.25 °C scenario is 1 cm less than the 2.0 °C scenario (table S-3), suggesting that GMST scenarios that are primarily represented by only one RCP (i.e. the 1.5 °C scenario) may be less sensitive to model filtering.

Agreement between central estimates from process-based and semi-empirical projections implies consistency with the observed statistical relationship between GMST and the rate of SLR used to calibrate the SESL model. Across scenarios, median 2100 GMSL projections from the SESL model driven with CMIP5 GMST trajectories are 7–8 cm lower than those from the K14 framework (figure 1 and table 1), but more disagreement exists between the processed-based and SESL projections when driven with the MAGICC GMST trajectories shown in SI, figure S-3 (median projection differences of 4–11 cm; table 1). These differences are smaller in magnitude relative to the differences in the median RCP2.6 and RCP4.5 projections from Kopp *et al* (2014) and the SESL projections from Kopp *et al* (2016a) (8–12 cm). After 2100, the differences between projections from the K14 framework and the SESL model become larger. Across scenarios, median 2200 GMSL projections from the K14 framework are higher by 34 cm (1.5 °C), 39 cm (2.0 °C) and 17 cm (2.5 °C) than those from the SESL model driven with CMIP5 GMST trajectories (figure 1 and table 1). These differences are largely attributed to the treatment of ice sheets in each approach. The K14 framework accounts for non-linearities in crossing threshold ice sheet behavior by drawing from AR5 and Bamber and Aspinall (2013), but the SESL model does not because these events are absent from the calibration period.

3.2. Population inundation

Under the median projected GMSL for a 2.0 °C GMST stabilization, lands currently home to about 60 million people are projected to be permanently submerged by 2150, including lands currently home to over half a million inhabitants of United Nations defined Small Island Developing States (SIDS). Aggregation of all SIDS can mask important risks. For instance, local SLR projections for 2150 under a 2.0 °C GMST stabilization place lands currently home to almost a quarter of the current population of the Marshall Islands at risk of being permanently submerged. In comparison to these totals, under the median projection for the 1.5 °C stabilization scenario, lands currently home to about 5 million people, including 60 000 in SIDS, avoid inundation (table 2), but little difference is found for the Marshall Islands.

3.3. Amplification of ESL events

We assess the effects of different GMST stabilizations on the frequency of ESL events by highlighting three cities: (1) New York, New York, USA, (2) Kushimoto, Wakayama, Japan, and (3) Cuxhaven, Lower Saxony, Germany (figure 2). Estimates of the historical 10-, 100-, and 500-year ESL events (expected frequency of 0.1/year, 0.01/year, and 0.002/year, respectively) and the future ESL frequency AF for all sites are provided in SI tables S-4 to S-6. Under 2.0 °C GMST stabilization, the 2100 median local SLR for New York City is 69 cm (*likely* 44–98 cm). In figure 2, median local SLR under the 2.0 °C scenario (SL_{50}) shifts the expected historic ESL event return curve to the right (i.e. $N(z)$, the heavy gray curve, becomes $N+SL_{50}$ 2.0 °C, the dashed green curve) and increases the expected annual number of historical 10 year ESL events from 0.1/year to ~10/year. However, when both the uncertainty in the GPD fit and the SLR projections are considered in the calculation of the projected future ESL event return curve (i.e. N_e 2.0 °C; the heavy green curve), the expected frequency of the current 10 year ESL event increases from 0.1/year to 36/year (i.e. 3/month, on average). GHG mitigation that

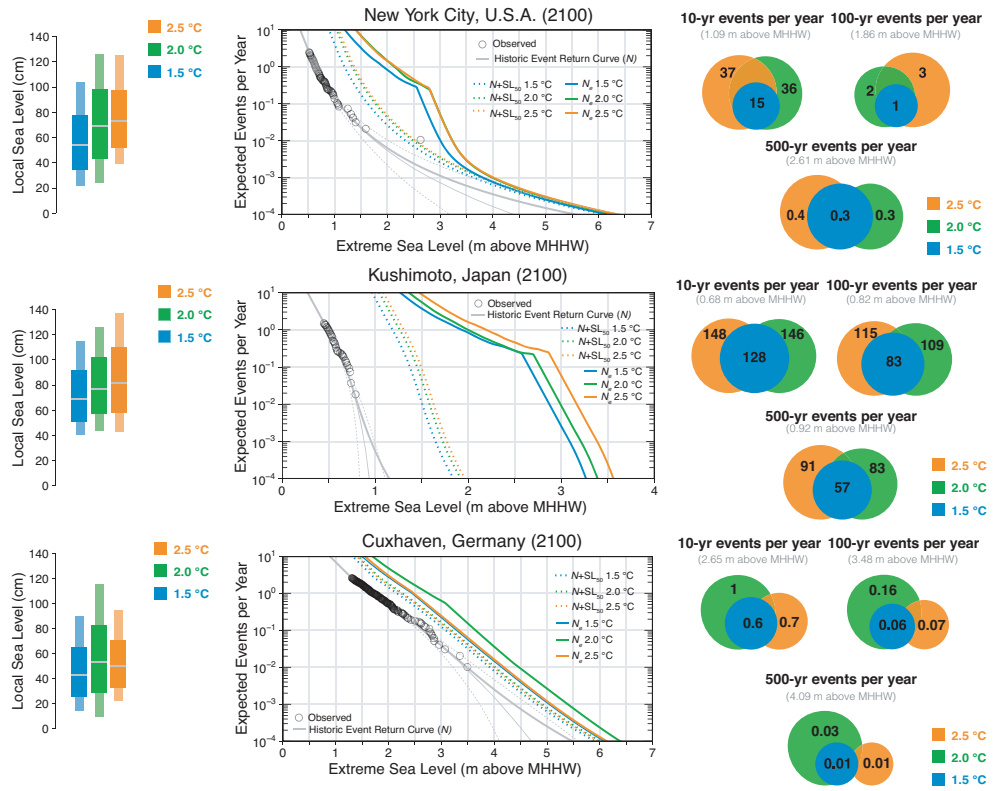

Figure 2. Top left: 2100 SLR (cm; relative to 2000) for New York City, USA, under 1.5 °C (blue), 2.0 °C (green), and 2.5 °C (orange) GMST stabilizations. Gray bars are median, heavy colors are 17/83 percentile and light shading is 5/95 percentile. Top middle: ESL event return curves for New York City indicating the relationship between the expected number of ESL events per year and ESL height (m above MHHW) for: 1) historical conditions (gray curves) and 2) year 2100 under both different GMST stabilizations (blue = 1.5 °C, green = 2.0 °C, orange = 2.5 °C) and consideration of local SLR uncertainty (dotted curves consider median SLR only (i.e. a fixed offset from N, $N + SL_{50}$); solid curves (N_e) incorporate local SLR projection uncertainty by integrating across both the entire SLR probability distribution and GPD parameter uncertainty; blue, green, and orange colors are the 1.5 °C, 2.0 °C, 2.5 °C scenarios, respectively). The thick gray curve is the expected historical ESL height return curve (N) that incorporates the uncertainty in the GPD parameter fit, open gray circles are observed ESL events from the tide gauge record, and thin grey lines are the historical ESL height return curves for the 17/50/83 percentiles of the GPD parameter uncertainty range (dotted/solid/dotted lines, respectively). The shape of the N_e curve varies by location in part because both local SLR uncertainty and the shape of the historical return curve vary by location. Top right: the expected number of ESL events per year by historical return period for New York City for 2100 under 1.5 °C (blue), 2.0 °C (green), and 2.5 °C (orange) GMST stabilization. Second row: as for top row, but for Kushimoto, Japan. Third row: as for top row, but for Cuxhaven, Germany.

stabilizes GMST at 1.5 °C reduces projected median local SLR at New York City to 55 cm (*likely* 35–78 cm), and reduces the expected number of current 10 year ESL events by half (15/year). By 2150, the reduction in projected 10 year ESL events from the 2.0 °C to the 1.5 °C scenario is still ~50% (99/year reduced to 59/year; table S-4).

Note that the expected number of flood events and the appearance of kinks in the N_e curves in figure 2 are sensitive to the way that the high-end tail of the mean sea level distributions are constructed. For example, for sample sizes explored in this study (<99.9th percentile), this truncation plays an important role in setting the location of the kinks in N_e and for sufficiently heavy tailed distributions, N_e may not converge within this range. Discontinuities in the N_e curves can also arise at the transition between modeling flood events with two different distributions. Specifically, expected ESL frequencies between the historical frequency of the GPD threshold exceedance (i.e. λ) and 182.6 events per year are modeled with a Gumbel distribution and expected ESL frequencies greater than λ are modeled with a GPD (section 2.4.1). Note that because the uncertainty in local SLR varies by location, the distance between the N+SL_{50} and N_e curves also differs by location.

Sea-level rise will amplify the frequency of all ESL events, but depending on the shape of the GPD, the frequency of some ESL events may amplify more than others (Buchanan *et al* 2017). For example, by 2100 under a 2.0 °C and 1.5 °C GMST stabilization, respectively, median local SLR for Kushimoto, Japan is projected to be 79 cm (*likely* 58–103 cm) and 70 cm (*likely* 52–92 cm), increasing the respective number of historical 10 year ESL events from 0.1/year, on average, to 146/year (AF of 1462) and 128/year (AF of 1277), on average. However, for the same amount of local SLR, the historical number of expected 500 year

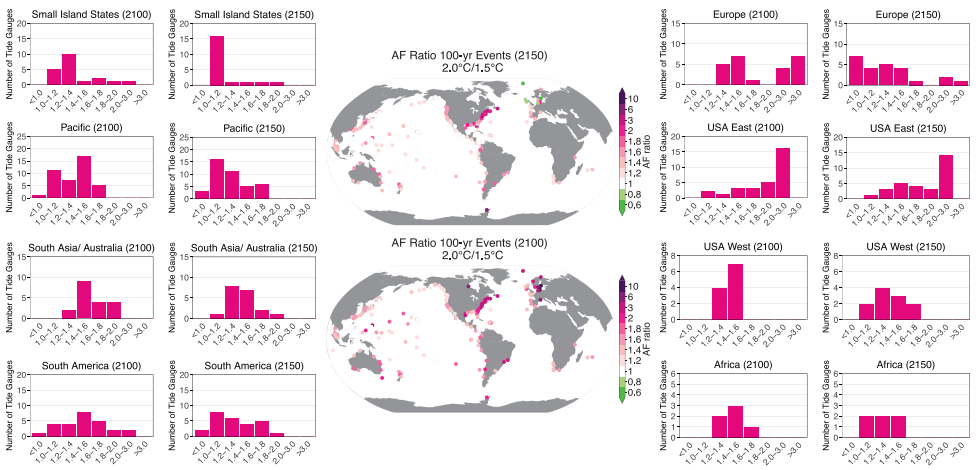

Figure 3. Maps: the ratio of ESL event AFs for historical 100 year ESL events between a 1.5 °C and 2.0 °C GMST stabilization target for the years 2150 (top) and 2100 (bottom). Larger 2.0 °C/1.5 °C AF ratios indicate where the historical 100 year ESL event occurs less often under 1.5 °C GMST stabilization than 2.0 °C GMST stabilization. Histograms: regionally binned ratios of 2.0 °C/1.5 °C expected AFs for the historical 100 year ESL event for 2100 and 2150. 'Small Island States' are United Nations defined Small Island Developing States. The list of tide gauges included in each region are given in table S-1 (SI).

ESL events for Kushimoto increases from 0.002/year to 83/year (2.0 °C; AF of 41479) and 57/year (1.5 °C; AF of 28 645). When the shape of the return curve is log-linear (as occurs when the shape parameter (ξ) is zero), ESL events amplify equally across return periods. For example, by 2100, under 1.5 °C, 2.0 °C, and 2.5 °C GMST stabilization, respectively, Cuxhaven, Germany is projected to have median local SLR of 43 cm (*likely* 26–65 cm), 53 cm (*likely* 29–82 cm) and 51 cm (*likely* 34–71 cm). The historical 500 year ESL event is projected to become as or more frequent than the historical 100 year ESL event for all scenarios: 0.01/year (1.5 °C; AF of 5.6), 0.03/year (2.0 °C; AF of 13.5), and 0.01/year (2.5 °C; AF of 6.5). Because the shape factor of the Cuxhaven GPD is close to zero, the historical 10 year ESL event also is projected to amplify similarly to the 500 year ESL event: 0.6/year (1.5 °C; AF of 5.6), 1.0/year (2.0 °C; AF of 13.5), and 0.7/year (2.5 °C; AF of 6.5). For some sites, including Cuxhaven, the AF for the 2.0 °C scenario may be greater than the AF for the 2.5 °C scenario. This can be partly attributed to higher SLR projections in the upper tail of the 2.0 °C probability distribution influencing the AF calculation.

We assess regional differences in 100 year ESL event frequency amplification between 2.0 °C and 1.5 °C GMST stabilization by binning ratios of 2.0 °C/1.5 °C expected AFs for 2100 and 2150 (figure 3). Bins on the right side of each graph become filled when there are decreases in the frequency of ESL events at regional groups of tide gauges from 1.5 °C over 2.0 °C GMST stabilization, while bins on the left side of each graph become filled when there are either no changes or increases in ESL event frequency at stations from 1.5 °C GMST over 2.0 °C GMST stabilization. In general, decreases in the frequency of ESL events from a 1.5 °C GMST stabilization grow as GMSL trajectories between scenarios separate from one another (table 1). By 2100 and 2150, substantial decreases in the frequency of ESL events from 1.5 °C GMST stabilization are expected in the East and Gulf Coasts of the United States, where ESL event amplification between GMST scenarios is reduced by roughly half. By 2150, smaller contributions from either local ocean dynamics or GICs in the 2.0 °C scenario attenuate SLR in parts of Europe, leading to lower median local SLR than from 1.5 °C GMST stabilization. Less local SLR in the 2.0 °C scenario causes ESL event frequencies to decrease, relative to the 1.5 °C scenario. We find small decreases or no change in ESL event frequency from achieving a 1.5 °C GMST stabilization over a 2.0 °C GMST stabilization at most tide gauges located in SIDS, as local SLR projections in these areas are similar between GMST scenarios (figure 3).

4. Discussion and conclusions

The Paris Agreement seeks to stabilize GMST by limiting warming to 'well below 2.0 °C above pre-industrial levels', but a recent literature review under the UNFCCC found the notion that 'up to 2.0 °C of warming is considered safe, is inadequate' and that 'limiting global warming to below 1.5 °C would come with several advantages' (UNFCCC 2015b). However, the location-specific increases in the frequency of ESLs illustrate the divergence between local and global perspectives on the question of what climate changes are 'dangerous'. The selection of a GMST target has important implications for long-term GMSL rise, ESLs, and consequently, coastal flooding. Assessing the distribution of impacts of incremental levels of warming

on ESLs is of relevance to >625 million people who currently reside in low-lying coastal areas (Neumann *et al* 2015) and are vulnerable to current and future ESL events. For countries without the economic and physical capacity to construct flood protection and flood-resilient infrastructure—including some recognized by the United Nations as SIDS—local SLR that results in permanent inundation and unmanageable flooding may threaten their existence (Wong *et al* 2014, Diaz 2016). The only feasible option for maintaining habitability for these locations may be the management of GMST through international climate accords, like the Paris Agreement, that govern the long-term committed rise in GMSL.

Only considering changes to the mean local sea level, we find that, under median projections, lands currently home to 5 million people will be spared from being permanently submerged by local mean sea levels by 2150 under a 1.5 °C GMST stabilization compared to local mean sea levels under the 2.0 °C case. This includes lands in SIDS currently home to 60 000 people (table 2). The effects of GMST stabilization on ESLs varies greatly by region and by historical return period (e.g. the 10 year versus the 100 year ESL event, etc). Globally, for the historical 100 year ESL event, we find that by 2100, the Eastern and Gulf coasts of the US and Europe could experience substantial benefits from a 1.5 °C GMST stabilization relative to a 2.0 °C GMST stabilization, with ESL frequency amplification being reduced by about half. However, while fractional reductions may appear substantial in some cases, small absolute differences may warrant similar coastal flood risk management responses. For instance, for New York City, we estimate the expected number of historical 100 year ESL events per year between a 2.0 °C to a 1.5 °C GMST stabilization is only two times and one time per year, respectively (figure 2).

While these data could be used in support of local probabilistic risk management strategies that intend to reduce current and future exposure and vulnerability to extreme flood events, some caveats should be highlighted. First, while our projections carry probabilities, these are not uniquely identifiable probabilities; ice sheet contributions in particular are deeply uncertain, so unique probability distributions for their future values do not exist (e.g. Kopp *et al* 2017). Moreover, our projections assume linear accelerations of ice-sheet contributions. Detailed physical models (e.g. Deconto and Pollard 2016) suggest that these approximations may fail over the course of the next three centuries. Rates of ice-sheet contributions may stabilize, or they may cross critical thresholds leading to non-linear accelerations. While the results of Deconto and Pollard (2016) suggest a critical threshold above 2 °C leading to considerably larger Antarctic contributions than at lower temperatures, estimates of the existence, location, and consequences of such thresholds are deeply uncertain. Second, we assume that the frequency of storm arrivals and their intensity will remain constant—and thus the Poisson and GPD parameters (section 2.4.1). Changes to storm frequency and severity could significantly influence future ESL events (e.g. Reed *et al* 2015, Emanuel 2013, Knutson *et al* 2010). Modifications could be made to include changes in these parameters with time (Ceres *et al* 2017). Third, these are projections of extreme high water at specific tide gauges and are not regional flood projections. Future flood projections are dependent on the dynamics of flood propagation, wave action, and future measures taken to reduce flood risk.

The selection of the level at which to stabilize the GMST in the coming years will determine the committed amounts of future GMSL (Clark *et al* 2016, Levermann *et al* 2013). Our projected coastal ESL impacts through the end of the 22nd century should be placed in the context of longer timeframes. Stabilization of GMST does not imply stabilization of GMSL. Regardless of the mitigation scenario chosen, GMSL rise due to thermal expansion is expected to continue for centuries to millennia. Additionally, some studies suggest that sustained GMST warming above given thresholds, potentially those as low as 1 °C, could lead to a near-complete loss of the GIS over a millennium or more (Robinson *et al* 2012). Coincident with continued GMSL rise will be further increases in the frequency of historical ESL events and an increasing number of currently inhabited lands that will be permanently submerged. A comprehensive approach to managing coastal flood risks would take into account changes on these very long timeframes.

Acknowledgments

We are grateful for comments from two anonymous reviewers and Carl-Friedrich Schleussner and colleagues at Climate Analytics. DJR and MKB were supported by the Science, Technology, and Environmental Policy (STEP) Program at Princeton. MO was supported in part by NSF EAR-1520683. REK was supported in part by a grant from Rhodium Group (for whom he has previously worked as a consultant), as part of the Climate Impact Lab consortium, and in part by NSF grant ICER-1663807 and by NASA grant 80NSSC17K0698. We acknowledge the World Climate Research Programme's Working Group on Coupled Modeling, which is responsible for CMIP, and we thank the climate modeling groups for producing and making available their model output (listed in SI table S-2). For CMIP, the US Department of Energy's Program for Climate Model Diagnosis and Intercomparison provides coordinating support and led development of software infrastructure in partnership with the Global Organization for Earth System Science Portals. Code for generating sea-level projections is available in the ProjectSL (https://github.com/bobkopp/ProjectSL), LocalizeSL (https://github.com/bobkopp/LocalizeSL),

and SESL (https://github.com/bobkopp/SESL) repositories on Github. Code for generating extreme sea level projections is available in the hawaiiSL_process (https://github.com/dmr2/hawaiiSL_process), GPDfit (https://github.com/dmr2/GPDfit), return_curves (https://github.com/dmr2/return_curves), and amplification (https://github.com/dmr2/amplification) repositories on Github. The statements, findings, conclusions, and recommendations are those of the authors and do not necessarily reflect the views of the funding agencies.

ORCID iDs

D J Rasmussen https://orcid.org/0000-0003-4668-5749
Maya K Buchanan https://orcid.org/0000-0001-9806-1132
Klaus Bittermann https://orcid.org/0000-0002-8251-6339
Benjamin H Strauss https://orcid.org/0000-0002-6856-6575
Robert E Kopp https://orcid.org/0000-0003-4016-9428
Michael Oppenheimer http://orcid.org/0000-0002-9708-5914

References

Bamber J L and Aspinall W P 2013 An expert judgement assessment of future sea level rise from the ice sheets *Nat. Clim. Change* **3** 424–7
Bittermann K, Rahmstorf S, Kopp R E and Kemp A C 2017 Global mean sea-level rise in a world agreed upon in Paris *Environ. Res. Lett.* **12** 124
Bright E A, Coleman P R, Rose A N and Urban M L 2011 LandScan 2010 Data Set
Buchanan M K, Kopp R E, Oppenheimer M and Tebaldi C 2016 Allowances for evolving coastal flood risk under uncertain local sea-level rise *Clim. Change* **137** 347–62
Buchanan M K, Oppenheimer M and Kopp R E 2017 Amplification of flood frequencies with local sea level rise and emerging flood regimes *Environ. Res. Lett.* **064009** 7
Caldwell P C, Merrifield M A and Thompson P R 2015 Sea level measured by tide gauges from global oceans—the Joint Archive for Sea Level holdings (NCEI Accession 0019568). NOAA National Centers for Environmental Information Dataset
Ceres R L, Forest C E and Keller K 2017 Understanding the detectability of potential changes to the 100 year peak storm surge *Clim. Change* **145** 221–35
Church J *et al* 2013 Sea level change *Clim. Chang. 2013 Phys. Sci. Basis. Contrib. Work. Gr. I to Fifth Assess. Rep. Intergov. Panel Clim. Change* ed T Stocker *et al* (Cambridge: Cambridge University Press) ch 13
Clark P U 2016 Consequences of twenty-first-century policy for multi-millennial climate and sea-level change *Nat. Clim. Change* **6** 360–9
Coles S 2001a Classical extreme value theory and models *Lecture Notes in Control and Information Sciences* (Berlin: Springer) ch 3
Coles S 2001b Threshold models *Lecture Notes in Control and Information Sciences* (Berlin: Springer) ch 4
Deconto R M and Pollard D 2016 Contribution of Antarctica to past and future sea-level rise *Nature* **531** 591–7
Diaz D B 2016 Estimating global damages from sea level rise with the coastal impact and adaptation model (ciam) *Clim. Change* **137** 143–56
Emanuel K A 2013 Downscaling CMIP5 climate models shows increased tropical cyclone activity over the st century *Proc. Natl Acad. Sci. USA* **110** 12219–24
Farrell W E and Clark J A 1976 On postglacial sea level *Geophys. J. R. Astron. Soc.* **46** 647–67
GISSTEMP Team 2017 GISS Surface Temperature Analysis (GISTEMP) (https://data.giss.nasa.gov/gistemp/)
Hansen J, Ruedy R, Sato M and Lo K 2010 Global surface temperature change *Rev. Geophys.* **48** rG4004
Held I M *et al* 2010 Probing the fast and slow components of global warming by returning abruptly to preindustrial forcing *J. Clim.* **23** 2418–27
Hijmans R 2012 GADM database of Global Administrative Areas 2.0 Data Set
Hinkel J *et al* 2014 Coastal flood damage and adaptation costs under 21st century sea-level rise *Proc. Natl Acad. Sci.* **111** 3292–7
Hsiang S *et al* 2017 Estimating economic damage from climate change in the United States *Science* **356** 1362–9
Hunter J 2012 A simple technique for estimating an allowance for uncertain sea-level rise *Clim. Change* **113** 239–52
Jackson L P, Grinsted A and Jevrejeva S 2018 21st century sea-level rise in line with the Paris accord *Earth's Future* **6** 2017EF000688
Jevrejeva S, Jackson L P, Riva R E M, Grinsted A and Moore J C 2016 Coastal sea level rise with warming above 2 °C *Proc. Natl Acad. Sci.* **113** 13342–7
Knutson T R *et al* 2010 Tropical cyclones and climate change *Nat. Geosci.* **3** 157–63
Kopp R E *et al* 2014 Probabilistic 21st and 22nd century sea-level projections at a global network of tide-gauge sites *Earth's Future* **2** 383–407
Kopp R E *et al* 2016a Temperature-driven global sea-level variability in the common Era *Proc. Natl Acad. Sci.* **113** E1434–41
Kopp R E, Shwom R L, Wagner G and Yuan J 2016b Tipping elements and climate–economic shocks: pathways toward integrated assessment *Earth's Future* **4** 346–72
Kopp R E *et al* 2017 Evolving understanding of antarctic ice-sheet physics and ambiguity in probabilistic sea-level projections **5** *Earth's Future* 2017EF000663
Kuhlbrodt T and Gregory J M 2012 Ocean heat uptake and its consequences for the magnitude of sea level rise and climate change *Geophys. Res. Lett.* **39** 1–6
Levermann A, Griesel A, Hofmann M, Montoya M and Rahmstorf S 2005 Dynamic sea level changes following changes in the thermohaline circulation *Clim. Dyn.* **24** 347–54
Levermann A *et al* 2013 The multimillennial sea-level commitment of global warming *Proc. Natl Acad. Sci* **110** 13745–50
Mann M E *et al* 2009 Global signatures and dynamical origins of the little ice age and medieval climate anomaly *Science* **326** 1256–60
Marzeion B and Levermann A 2014 Loss of cultural world heritage and currently inhabited places to sea-level rise *Environ. Res. Lett.* **9** 034
Marzeion B, Jarosch A H and Hofer M 2012 Past and future sea-level change from the surface mass balance of glaciers *Cryosphere* **6** 1295–322
Meinshausen M, Raper S C B and Wigley T M L 2011a Emulating coupled atmosphere-ocean and carbon cycle models with a simpler model, magicc6—part 1: Model description and calibration *Atmos. Chem. Phys.* **11** 1417–56
Meinshausen M *et al* 2011b The {RCP} greenhouse gas concentrations and their extensions from 1765–2300 *Clim. Change* **109** 213–41
Milne G A, Gehrels W R, Hughes C W and Tamisiea M E 2009 Identifying the causes of sea-level change *Nat. Publ. Gr.* **2** 471–8
Mitchell D *et al* 2017 Half a degree additional warming, prognosis and projected impacts (HAPPI): background and experimental design *Geosci. Model Dev.* **10** 571–83

Mitrovica J X et al 2011 On the robustness of predictions of sea level fingerprints *Geophys. J. Int.* **187** 729–42
Mohammed K et al 2017 Extreme flows and water availability of the Brahmaputra river under 1.5 °C and 2 °C global warming scenarios *Clim. Change* **145** 159–75
Moss R H et al 2010 The next generation of scenarios for climate change research and assessment *Nature* **463** 747–56
NASA JPL 2013 NASA Shuttle Radar Topography Mission Global 1 arc second [Data set] NASA LP DAAC
Neumann B, Vafeidis A T, Zimmermann J and Nicholls R J 2015 Future coastal population growth and exposure to sea-level rise and coastal flooding—a global assessment *PLoS ONE* **10**
Perrette M, Landerer F, Riva R, Frieler K and Meinshausen M 2013 A scaling approach to project regional sea level rise and its uncertainties *Earth Syst. Dyn.* **4** 11–29
Rahmstorf S 2007 A semi-empirical approach to projecting future sea-level rise *Science* **315** 368–70
Rahmstorf S, Perrette M and Vermeer M 2012 Testing the robustness of semi-empirical sea level projections *Clim. Dyn.* **39** 861–75
Raper S C B, Gregory J M and Stouffer R J 2002 The role of climate sensitivity and ocean heat uptake on AOGCM transient temperature response *J. Clim.* **15** 124–30
Rasmussen D J, Meinshausen M and Kopp R E 2016 Probability-weighted ensembles of US county-level climate projections for climate risk analysis *J. Appl. Meteorol. Climatol.* **55** 2301–22
Reed A J et al 2015 Increased threat of tropical cyclones and coastal flooding to New York City during the anthropogenic era *Proc. Natl Acad. Sci.* **112** 12610–5
Robinson A, Calov R and Ganopolski A 2012 Multistability and critical thresholds of the greenland ice sheet *Nat. Clim. Change* **2** 429–32
Schaeffer M, Hare W, Rahmstorf S and Vermeer M 2012 Long-term sea-level rise implied by 1.5 °C and 2 °C warming levels *Pro. Natl Acad. Sci.* **2** 867–70
Schleussner C F et al 2016a Differential climate impacts for policy-relevant limits to global warming: the case of 1.5 °C and 2 °C *Earth Syst. Dyn.* **7** 327–51
Schleussner C F et al 2016b Science and policy characteristics of the Paris agreement temperature goal *Nat. Clim. Change* **6** 827–35
Strauss B H, Kulp S and Levermann A 2015 Mapping choices: carbon, climate, and rising seas, our global legacy *Climate Central Report* pp 1–38
Sweet W V and Park J 2014 From the extreme to the mean: Acceleration and tipping points of coastal inundation from sea level rise *Earth's Future* **2** 579–600
Taylor K E, Stouffer R J and Meehl G A 2012 An overview of CMIP5 and the experiment design *Bull. Am. Meteorol. Soc.* **93** 485–98
Tebaldi C, Strauss B H and Zervas C E 2012 Modelling sea level rise impacts on storm surges along US coasts *Environ. Res. Lett.* **7** 14–32
UNFCCC 1992 *The United Nations Framework Convention on Climate Change* (New York: United Nations)
UNFCCC 2015a *Report of the Conference of the Parties on Its Twenty-First Session, Held in Paris from 30 November–13 December 2015* (New York: United Nations)
UNFCCC 2015b *Report on the Structured Expert Dialogue on the 2013-2015 Review* (New York: United Nations)
Vermeer M and Rahmstorf S 2009 Global sea level linked to global temperature *Proc. Natl Acad. Sci.* **106** 21527–32
van Vuuren D P et al 2011 The representative concentration pathways: an overview *Clim. Change* **109** 5
Wahl T et al 2017 Understanding extreme sea levels for broad-scale coastal impact and adaptation analysis *Nat. Commun.* **8** 16075
Wong P P et al 2014 *Coastal Systems and Low-Lying Areas* (Cambridge: Cambridge University Press) pp 361–409

Supplementary Information

S-1 Preparation of tide gauge data for extreme value analysis

Tide gauge observations are prepared as the basis for extreme value analysis following the methods of Tebaldi et al (2012). First, daily maximum tide gauge values are calculated from the "Research Quality" hourly observations from the University of Hawaii Sea Level Center (retrieved from: https://uhslc.soest.hawaii.edu/, June 2017; Caldwell et al, 2015). We only use tide gauges with record lengths $\geq$ 30 years and $\geq$ 80 percent data completion within each record therein. A list of tide gauges and the portion of their records used in this study is provided in Table S-1.

The long-term trend in sea-level change over the tide gauge record is removed to isolate the impact on sea levels from day-to-day weather, astronomical tides and seasonal cycles. Specifically, monthly mean sea levels over the tide gauge record are used to linearly de-trend the daily maximum observations. The de-trended daily maximum observations are then registered to the mean higher high water (MHHW) height at each tide gauge. At each tide gauge, the MHHW height is estimated using the average of the daily maximum tide gauge observations over the most recent 19-year period in the tide gauge record. While the MHHW calculation approach differs from the current U.S. standard (which is defined over the National Tidal Datum Epoch of 1983–2001), it is done after de-trending of the daily time series and should therefore be close to stationary.

Finally, at each tide gauge the daily maximum observations above the 99th percentile are de-clustered to separate multiple observations made during the same extreme sea level event and so that each observation used to estimate the extreme value distribution is statistically independent of one another. The 99th percentile is used as it is generally above the highest seasonal tide and it balances the bias-variance trade-off in the GPD parameter estimation. If too low of a GPD threshold is chosen, more observations than those exclusively in the tail of the GPD distribution might end up being included in the parameter calculation, causing bias. If too high of a GPD threshold is chosen, then too few observations may be incorporated in the estimation of distribution parameters leading to greater variance, relative to a case that uses more observations.

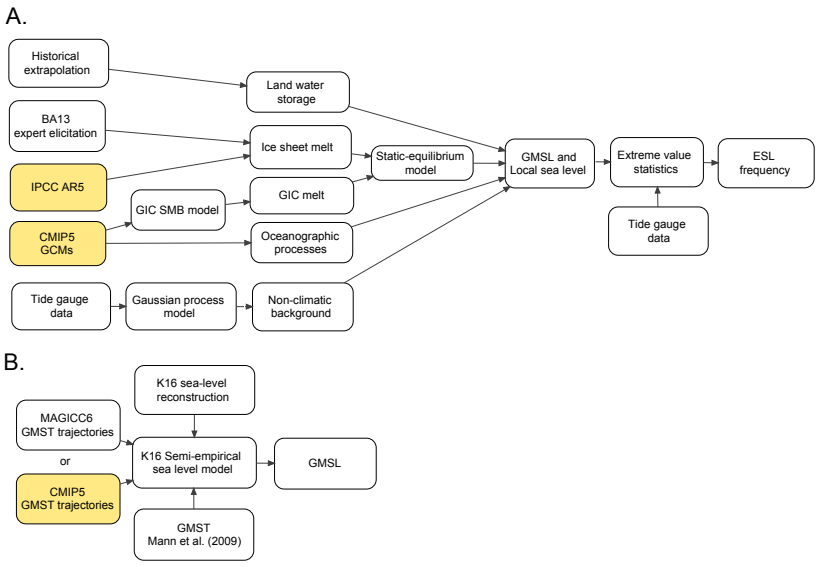

Fig. S-1 Top: Logical flow of sources of information used in local sea-level projections and extreme sea level (ESL) event return curves. GCMs are global climate models; GIC is glaciers and ice caps; SMB is surface mass balance; GMST is global mean surface temperature; GMSL is global mean sea level; BA13 is Bamber and Aspinall, 2013; K16 is Kopp et al, 2016a. Orange shades indicate where RCP and model grouping occurs (see Table S-2). **Bottom:** Logical flow of sources of information used to construct semi-empirical GMSL projections. Note that either the MAGICC6 or CMIP5 GMST trajectories can be used to drive the semi-empirical sea level model.

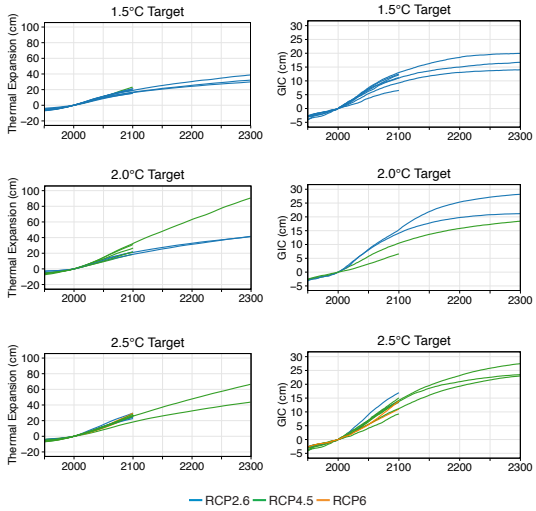

Fig. S-2 Left Column: Thermal expansion contribution to global mean sea-level (GMSL) rise (cm; relative to 2000) from CMIP5 models that have been smoothed and corrected for model drift for global mean surface temperature stabilization targets of 1.5 °C, 2.0 °C, and 2.5 °C (blue = RCP2.6, green = RCP4.5, orange = RCP6). **Right Column:** As for Left Column, but for glaciers and ice cap (GIC) contributions to GMSL rise (cm; relative to 2000) using the model from Marzeion et al (2012). Table S-2 lists the models used for each temperature target.

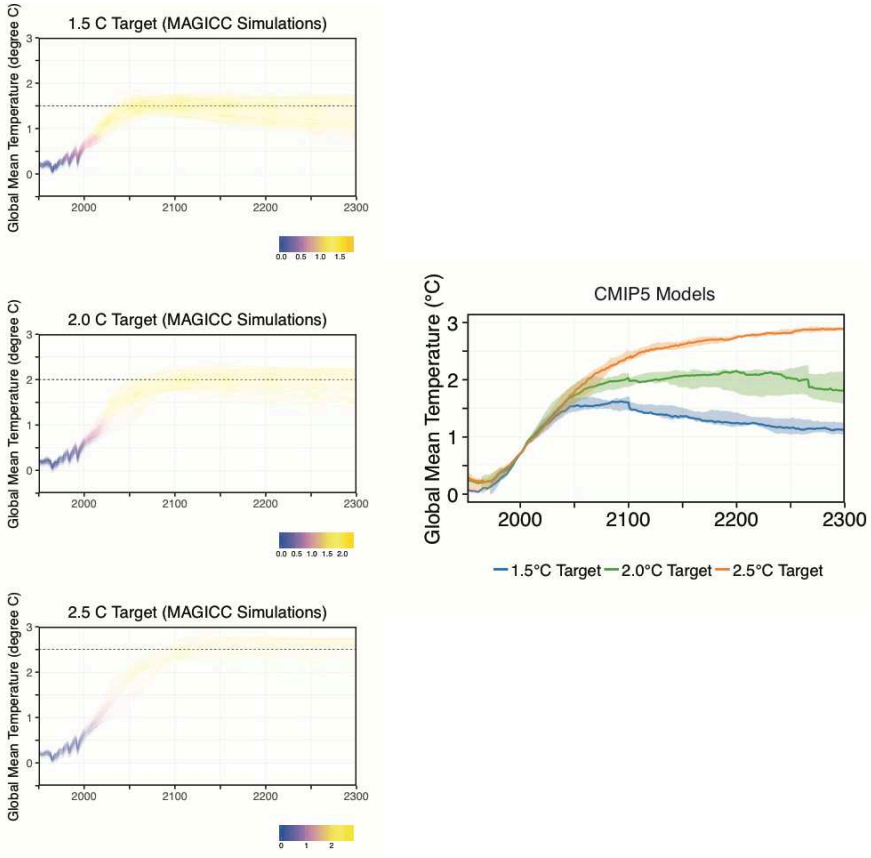

Fig. S-3 Left: Global mean temperature trajectories from MAGICC6 that have a 2100 GMST of 1.5 °C, 2.0 °C, and 2.5 °C ± 0.25°C (relative to 1875–1900). Temperatures are relative to 1875–1900. **Right:** Global mean surface temperature (GMST) trajectories from CMIP5 models (1950–2300) that have a 2100 GMST of 1.5 °C, 2.0 °C, and 2.5 °C ± 0.25°C (relative to 1875–1900). GMST is anomalized to 1991–2009 and shifted up by 0.72°C to account for warming since 1875–1900 (Hansen et al, 2010; GISSTEMP Team, 2017). Solid line is the 50th percentile and shading is the 17th/83rd range.

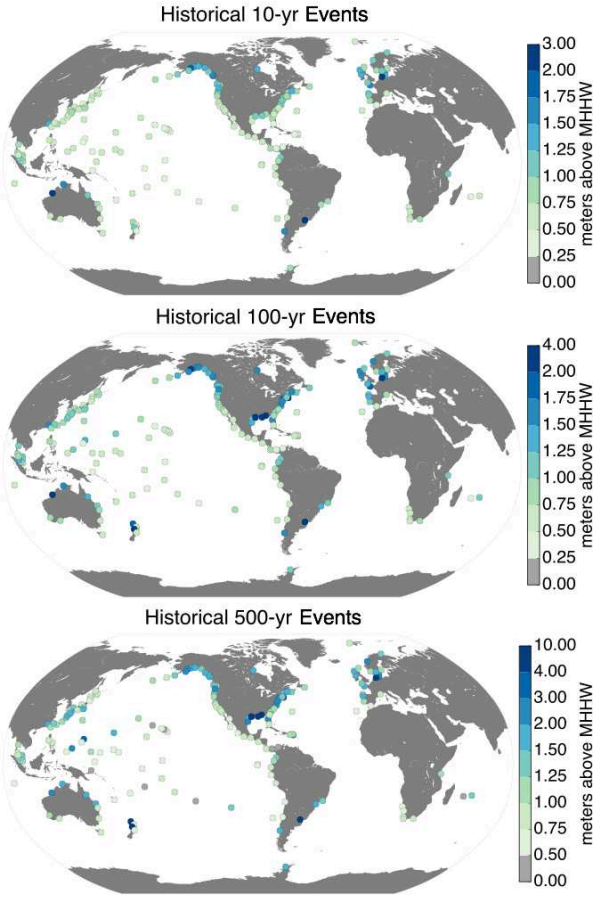

Fig. S-4 Historical extreme sea level height [meters above mean higher high water (MHHW)] for return periods of 10-, 100-, and 500-years.

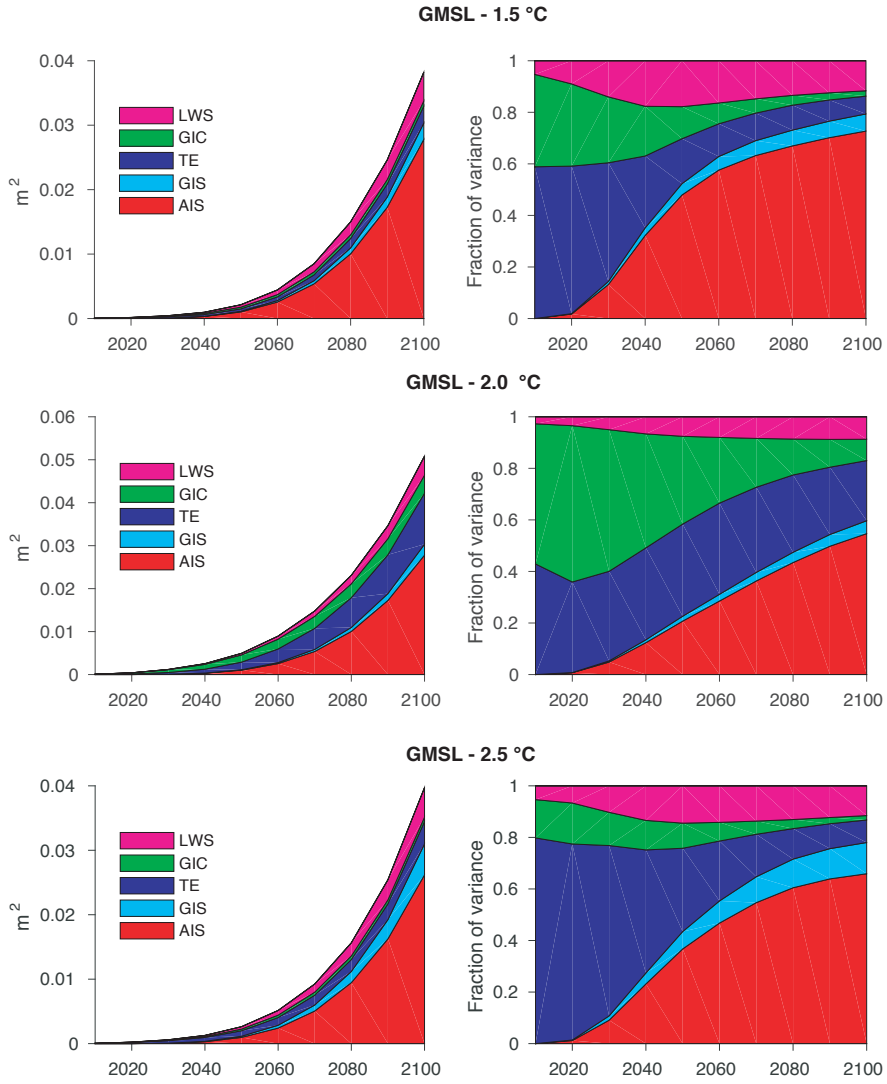

Fig. S-5 Global mean sea level (GMSL) sources of variance in raw and fractional terms in 1.5 °C, 2.0 °C, and 2.5 °C global mean surface temperature stabilization scenarios. AIS: Antarctic ice sheet, GIS: Greenland ice sheet, TE: thermal expansion, GIC: glaciers and ice caps, LWS: land water storage

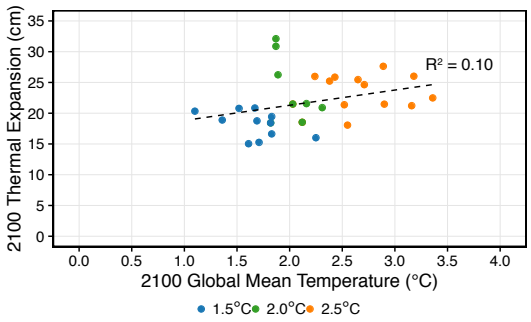

Fig. S-6 Relationship between 2100 global mean thermal expansion contribution to sea-level rise (i.e., 'zostoga') (cm) and the 19-yr running average of global mean surface temperature (GMST) for 2100 from CMIP5 model output (°C, relative to 1875–1900) under 1.5 °C (blue), 2.0 °C (green), and 2.5 °C (orange) GMST stabilization scenarios. Black dotted line is the linear fit across all temperature scenarios and all models.

Table S-1: List of tide gauges used from the University of Hawaii Sea Level Center and their record lengths.

Site	Country	Region	Lat	Lon	UHawaii ID	Start	End	Length (yrs)
Buenos Aires	Argentina	South America	-34.67	-58.50	285a	1905	1961	57
Fort Denison	Australia	South Asia/ Australia	-33.90	151.32	333a	1965	2015	51
Bundaberg	Australia	South Asia/ Australia	-24.77	152.50	332a	1984	2015	32
Brisbane	Australia	South Asia/ Australia	-27.37	153.17	331a	1984	2015	32
Spring Bay	Australia	South Asia/ Australia	-42.67	148.07	335a	1985	2015	31
Townsville	Australia	South Asia/ Australia	-19.25	146.83	334a	1984	2013	30
Broome	Australia	South Asia/ Australia	-18.02	122.23	166a	1986	2015	30
Cocos	Australia	South Asia/ Australia	-12.12	96.97	171a	1985	2015	31
Darwin	Australia	South Asia/ Australia	-12.52	130.97	168a	1984	2015	32
Esperance	Australia	South Asia/ Australia	-33.90	122.02	176a	1985	2015	31
Fremantle	Australia	South Asia/ Australia	-32.05	115.73	175a	1984	2015	32
Cananeia	Brazil	South America	-25.02	-48.00	281a	1954	2006	53
Ilha Fiscal, RJ	Brazil	South America	-23.02	-43.30	280a	1963	2012	50
Victoria, BC	Canada	Canada	48.50	-123.40	543a	1909	2014	106
Prince Rupert	Canada	Canada	54.32	-130.38	540a	1924	2014	91
Tofino	Canada	Canada	49.18	-126.03	542a	1930	2014	85
St. John's-A	Canada	Canada	47.57	-52.70	276a	1952	1989	38
Halifax	Canada	Canada	44.67	-63.58	275a	1899	2014	116
Churchill	Canada	Canada	58.77	-94.18	274a	1961	2012	52
Puerto Montt	Chile	South America	-41.50	-73.07	684a	1980	2014	35
Juan Fernandez-B	Chile	South America	-33.67	-78.95	021b	1985	2014	30
Antofagasta	Chile	South America	-23.68	-70.45	080a	1945	2014	70
Easter-C	Chile	South America	-27.20	-109.50	022c	1970	2014	45
Valparaiso	Chile	South America	-33.12	-71.72	081a	1944	2014	71
Xiamen	China	Pacific	24.45	118.07	376a	1954	1997	44
Buenaventura	Colombia	South America	3.95	-77.17	085a	1953	2014	62
Tumaco	Colombia	South America	1.82	-78.85	303a	1951	2014	64
Cartagena	Colombia	South America	10.38	-75.53	265a	1951	1993	43
Penrhyn	Cook Islands	SIDS	-9.07	-158.08	024a	1977	2015	39
Quepos-A	Costa Rica	South America	9.40	-84.17	087a	1961	1994	34
Hornbaek	Denmark	Europe	56.10	12.47	838a	1891	2012	122
Gedser	Denmark	Europe	54.57	11.93	837a	1891	2012	122
Baltra-B	Ecuador	South America	-0.47	-90.30	003b	1985	2015	31
Santa Cruz	Ecuador	South America	-0.80	-90.43	030a	1978	2015	38
La Libertad	Ecuador	South America	-2.20	-80.92	091a	1949	2015	67
Acajutla-A	El Salvador	South America	13.58	-89.83	082a	1962	2001	40
Chuuk	Fd. St. Micronesia	SIDS	7.45	151.85	054a	1956	1991	36
Kapingamarangi	Fd. St. Micronesia	SIDS	1.23	154.87	029a	1978	2015	38
Pohnpei-B	Fd. St. Micronesia	SIDS	7.02	158.33	001b	1974	2004	31
Yap-B	Fd. St. Micronesia	SIDS	9.58	138.23	008b	1969	2015	47
Suva-C	Fiji	SIDS	-18.27	178.52	018c	1972	2015	44
Noumea	France	Europe	-22.32	166.42	019a	1967	2015	49
Brest	France	Europe	48.38	-4.60	822a	1846	2014	169
Marseille	France	Europe	43.38	5.38	824a	1885	1988	104
Rikitea	French Polynesia	SIDS	-23.20	-134.98	016a	1969	2015	47
Papeete-B	French Polynesia	SIDS	-17.60	-149.57	015b	1975	2015	41
Cuxhaven	Germany	Europe	53.87	8.72	825a	1917	2014	98
Malin Head	Ireland	Europe	55.37	-7.33	834a	1958	2001	44
Hakodate	Japan	Pacific	41.78	140.72	364a	1964	2014	51
Hamada	Japan	Pacific	34.90	132.07	348a	1984	2014	31
Maisaka	Japan	Pacific	34.68	137.62	356a	1968	2014	47
Ishigaki	Japan	Pacific	24.33	124.15	365a	1969	2014	46
Naha	Japan	Pacific	26.22	127.67	355a	1966	2014	49
Toyama	Japan	Pacific	36.77	137.23	349a	1967	2014	48
Hosojima	Japan	Pacific	32.42	131.68	358a	1933	1975	43
Kushiro	Japan	Pacific	42.97	144.37	350a	1963	2014	52
Abashiri	Japan	Pacific	44.02	144.28	347a	1968	2014	47
Mera	Japan	Pacific	34.92	139.82	352a	1965	2014	50
Wakkanai	Japan	Pacific	45.40	141.68	360a	1967	2014	48
Chichijima	Japan	Pacific	27.10	142.18	047a	1975	2014	40
Nishinoomote	Japan	Pacific	30.75	131.07	363a	1965	2013	49
Naze	Japan	Pacific	28.52	129.60	359a	1957	2013	57
Hachinohe	Japan	Pacific	40.53	141.53	375a	1980	2011	32
Miyakejima	Japan	Pacific	34.07	139.62	357a	1964	2013	50
Nakano Shima	Japan	Pacific	29.92	129.92	345a	1984	2013	30

Continued on next page

Table S-1 – continued from previous page

Site	Country	Region	Lat	Lon	UHawaii ID	Start	End	Length (yrs)
Ofunato	Japan	Pacific	39.02	141.75	351a	1965	2014	50
Nagasaki	Japan	Pacific	32.73	129.87	362a	1985	2014	30
Aburatsu	Japan	Pacific	31.58	131.42	354a	1961	2014	54
Kushimoto	Japan	Pacific	33.48	135.77	353a	1961	2014	54
Cendering	Malaysia	South Asia/ Australia	5.40	103.22	320a	1984	2013	30
Johor Baharu	Malaysia	South Asia/ Australia	1.57	103.87	321a	1983	2013	31
Kuantan	Malaysia	South Asia/ Australia	4.05	103.55	322a	1983	2013	31
Keling	Malaysia	South Asia/ Australia	2.35	102.18	141a	1984	2013	30
Lumut	Malaysia	South Asia/ Australia	4.30	100.73	143a	1984	2013	30
Kelang	Malaysia	South Asia/ Australia	3.05	101.43	140a	1983	2013	31
Langkawi	Malaysia	South Asia/ Australia	6.90	99.80	142a	1985	2015	31
Penang	Malaysia	South Asia/ Australia	5.47	100.47	144a	1984	2013	30
Port Louis-C	Mauritius	SIDS	-20.20	57.60	103c	1986	2015	30
Rodrigues	Mauritius	SIDS	-19.68	63.43	105a	1986	2015	30
Manzanillo-A	Mexico	South America	19.08	-104.45	395a	1953	1982	30
Ensenada	Mexico	South America	31.85	-116.63	317a	1956	1991	36
Salina Cruz	Mexico	South America	16.25	-95.23	394a	1952	1983	32
Acapulco-A, Gro.	Mexico	South America	16.90	-100.02	316a	1952	1995	44
Cabo San Lucas	Mexico	South America	23.00	-109.98	034a	1973	2002	30
Guaymas	Mexico	South America	27.93	-110.90	397a	1953	1986	34
Saipan-B	N. Mariana Islands	SIDS	15.32	145.82	028b	1978	2015	38
Marsden Point	New Zealand	South Asia/ Australia	-35.83	174.50	398a	1975	2014	40
Tauranga	New Zealand	South Asia/ Australia	-37.65	176.18	073a	1984	2014	31
Taranaki	New Zealand	South Asia/ Australia	-39.05	174.03	076a	1984	2014	31
Wellington	New Zealand	South Asia/ Australia	-41.28	174.78	071a	1944	2014	71
Tregde	Norway	Europe	58.00	7.57	804a	1927	2008	82
Rorvik	Norway	Europe	64.87	11.25	803a	1969	2014	46
Ny-Alesund	Norway	Europe	78.93	11.95	823a	1976	2014	39
Vardo	Norway	Europe	70.33	31.10	805a	1979	2014	36
Balboa	Panama	South America	9.10	-79.63	302a	1907	2014	108
Cristobal	Panama	South America	9.40	-80.05	266a	1907	2014	108
Rabaul	Papua New Guinea	SIDS	-4.20	152.25	010a	1966	1997	32
Lobos de Afuera	Peru	South America	-6.93	-80.72	084a	1982	2014	33
Callao-B	Peru	South America	-12.08	-77.17	093b	1970	2015	46
Legaspi	Philippines	Pacific	13.25	123.83	371a	1984	2015	32
Manila	Philippines	Pacific	14.60	120.98	370a	1984	2015	32
Cascais	Portugal	Europe	38.77	-9.42	209a	1959	2005	47
Funchal-B	Portugal	Europe	32.73	-17.03	218b	1982	2013	32
Kanton-B	Rep. of Kiribati	SIDS	-2.90	-171.73	013b	1972	2012	41
Christmas-B	Rep. of Kiribati	SIDS	2.12	-157.52	011b	1974	2015	42
Majuro-A	Rep. of Marshall I	SIDS	7.17	171.43	005a	1968	1999	32
Kwajalein	Rep. of Marshall I	SIDS	8.73	167.73	055a	1946	2014	69
Malakal-B	Republic of Belau	SIDS	7.45	134.58	007b	1969	2015	47
Kaohsiung	Republic of China	Pacific	22.75	120.33	340a	1980	2014	35
Keelung	Republic of China	Pacific	25.22	121.85	341a	1980	2014	35
Luderitz	South Africa	Africa	-26.65	15.15	702a	1958	1995	38
Saldahna Bay	South Africa	Africa	-33.02	17.95	703a	1982	2011	30
Simon's Town	South Africa	Africa	-34.18	18.43	221a	1959	1999	41
Port Nolloth	South Africa	Africa	-29.25	16.87	701a	1958	1997	40
Port Elizabeth	South Africa	Africa	-34.05	25.75	184a	1978	2014	37
La Coruna	Spain	Europe	43.37	-8.40	830a	1943	2013	71
Ceuta	Spain	Europe	35.90	-5.32	207a	1944	2013	70
Vigo	Spain	Europe	42.23	-8.73	208a	1943	1990	48
Stockholm	Sweden	Europe	59.40	18.22	826a	1889	2014	126
Goteborg-Torsh.	Sweden	Europe	57.70	11.85	819a	1967	2014	48
Zanzibar	Tanzania	Africa	-6.20	39.25	151a	1984	2015	32
Ko Lak	Thailand	South Asia/ Australia	11.90	99.82	328a	1985	2015	31
Stornoway	United Kingdom	Europe	58.28	-6.43	295a	1976	2010	35
Lerwick	United Kingdom	Europe	60.20	-1.20	293a	1959	2010	52
Faraday	United Kingdom	Europe	-65.25	-64.27	700a	1978	2013	36
Gibraltar-A	United Kingdom	Europe	36.13	-5.35	289a	1961	1992	32
Bermuda-B	United Kingdom	Europe	32.43	-64.73	259b	1985	2014	30
Newlyn, Cornwall	United Kingdom	Europe	50.12	-5.62	294a	1915	2010	96
Seward-C, AK	USA	Canada	60.15	-149.52	560c	1967	2014	48
Ketchikan, AK	USA	Canada	55.33	-131.70	571a	1937	2014	78
Valdez, AK	USA	Canada	61.20	-146.47	562a	1973	2014	42
Yakutat, AK	USA	Canada	59.68	-139.75	570a	1961	2014	54
Seldovia, AK	USA	Canada	59.50	-151.75	561a	1975	2014	40

Continued on next page

Table S-1 – continued from previous page

Site	Country	Region	Lat	Lon	UHawaii ID	Start	End	Length (yrs)
Sitka, AK	USA	Canada	57.07	-135.42	559a	1938	2014	77
Sand Point, AK	USA	Canada	55.37	-160.52	574a	1973	2014	42
Dutch Harbor-B, AK	USA	Canada	54.00	-166.57	041b	1982	2014	33
Cordova-B, AK	USA	Canada	60.63	-145.78	583b	1964	2014	51
Kodiak Isl., AK	USA	Canada	57.87	-152.62	039a	1975	2014	40
Adak, AK	USA	Canada	51.98	-176.77	040a	1950	2014	65
San Francisco, CA	USA	USA West	37.87	-122.60	551a	1897	2014	118
San Diego, CA	USA	USA West	32.83	-117.23	569a	1906	2014	109
Los Angeles, CA	USA	USA West	33.75	-118.32	567a	1923	2014	92
Crescent City, CA	USA	USA West	41.85	-124.18	556a	1933	2014	82
Monterey, CA	USA	USA West	36.65	-121.93	555a	1973	2014	42
Port San Luis, CA	USA	USA West	35.27	-120.85	565a	1948	2014	67
Santa Monica, CA	USA	USA West	34.08	-118.50	578a	1973	2014	42
La Jolla, CA	USA	USA West	32.87	-117.32	554a	1924	2014	91
New London, CT	USA	USA East	41.40	-72.12	744a	1938	2014	77
Lewes, DE	USA	USA East	38.92	-75.15	747a	1957	2014	58
Fernandina Beach, FL	USA	USA East	30.72	-81.47	240a	1897	1930	34
St. Petersburg, FL	USA	USA East	27.85	-82.72	759a	1946	2014	69
Pensacola, FL	USA	USA East	30.43	-87.33	762a	1923	2014	92
Mayport, FL	USA	USA East	30.50	-81.57	753a	1928	2000	73
Limetree Bay, FL	USA	USA East	17.82	-64.78	254a	1982	2014	33
Key West, FL	USA	USA East	24.58	-81.88	242a	1913	2014	102
Fort Pulaski, GA	USA	USA East	32.03	-80.92	752a	1935	2014	80
Hilo, HI	USA	Pacific	19.73	-155.07	060a	1927	2014	88
French Frigate, HI	USA	Pacific	23.88	-166.33	014a	1974	2007	34
Kahului, HI	USA	Pacific	20.90	-156.47	059a	1950	2014	65
Mokuoloe, HI	USA	Pacific	21.43	-157.80	061a	1957	2014	58
Honolulu-B, HI	USA	Pacific	21.37	-157.87	057b	1905	2014	110
Nawiliwili, HI	USA	Pacific	21.97	-159.35	058a	1954	2014	61
Grand Isle, LA	USA	USA East	29.38	-90.02	765a	1980	2014	35
Woods Hole, MA	USA	USA East	41.58	-70.72	742a	1957	2014	58
Nantucket, MA	USA	USA East	41.30	-70.22	743a	1965	2014	50
Boston, MA	USA	USA East	42.40	-71.07	741a	1921	2014	94
Portland, ME	USA	USA East	43.72	-70.37	252a	1910	2014	105
Eastport, ME	USA	USA East	44.93	-67.00	740a	1929	2014	86
Duck Pier, NC	USA	USA East	36.18	-75.87	260a	1978	2014	37
Wilmington, NC	USA	USA East	34.32	-77.98	750a	1935	2014	80
Atlantic City, NJ	USA	USA East	39.40	-74.43	264a	1911	2014	104
Cape May, NJ	USA	USA East	38.98	-75.05	746a	1965	2014	50
Montauk, NY	USA	USA East	41.18	-72.05	279a	1959	2014	56
New York, NY	USA	USA East	40.70	-74.15	745a	1920	2014	95
Charleston, OR	USA	USA West	43.45	-124.37	575a	1978	2014	37
South Beach, OR	USA	USA West	44.70	-124.13	592a	1967	2014	48
Astoria, OR	USA	USA West	46.28	-123.77	572a	1925	2014	90
Newport, RI	USA	USA East	41.55	-71.42	253a	1930	2014	85
Charleston, SC	USA	USA East	32.92	-80.00	261a	1921	2014	94
Rockport, TX	USA	USA East	28.07	-97.17	769a	1944	2014	71
Port Isabel, TX	USA	USA East	26.15	-97.35	772a	1977	2014	38
Chesapeake BBT, VA	USA	USA East	36.97	-76.23	749a	1975	2014	40
Neah Bay, WA	USA	USA East	48.38	-124.62	558a	1934	2014	81
Willapa Bay, WA	USA	USA East	46.78	-124.10	564a	1972	2014	43
Galveston, Pier 21, TX	USA	USA East	29.40	-94.88	775a	1904	2014	111
Galveston, P. Pier, TX	USA	USA East	29.32	-94.85	767a	1957	2011	55
Apra Harbor, Guam	USA Trust	Pacific	13.43	144.65	053a	1948	2014	67
Wake	USA Trust	Pacific	19.28	166.62	051a	1950	2014	65
Johnston	USA Trust	Pacific	16.78	-169.65	052a	1947	2015	69
Midway	USA Trust	Pacific	28.22	-177.37	050a	1947	2014	68
Pago Pago	USA Trust	Pacific	-14.28	-170.68	056a	1948	2014	67
Charlotte Amalie, VI	USA Trust	SIDS	18.35	-64.95	255a	1978	2014	37
San Juan, PR	USA Trust	SIDS	18.55	-66.12	245a	1977	2014	38
Magueyes Island, PR	USA Trust	SIDS	18.02	-67.17	246a	1965	2014	50

Table S-2 Inventory of CMIP5 models and their RCPs used for 1.5 °C, 2.0 °C, and 2.5 °C global mean surface temperature (GMST) stabilization targets. Information is given for the 19-yr running average 2100 GMST (°C; relative to 1875–1900), the lengths of the GMST projections, and the models used for generating contributions to global and local sea-level change from oceanographic processes and glaciers and ice caps (GIC; from Marzeion et al (2012)). 'Ocean Dynamics' is the local dynamic sea surface height anomaly (i.e., CMIP5 model output variable 'zos'; used only for local sea level projections) and 'Thermal Expansion' refers to the contribution to the change in the global mean sea level due to thermal expansion (i.e., CMIP5 model output variables 'zostoga' and 'zosga'). For the global average sea level projections, only the 'Thermal Expansion' component is considered, while local sea level projections use both the 'Ocean Dynamics' and 'Thermal Expansion' components.

1.5 °C

Model	RCP	2100 GMST (°C)	GMST	Ocean Dynamics	Thermal Expansion	GIC
bcc-csm1-1	RCP 2.6	1.51	23	23	23	23
BNU-ESM	RCP 2.6	1.62	21			
CCSM4	RCP 2.6	1.45	23	23	21	21
FIO-ESM	RCP 4.5	1.7	21	21		
GFDL-ESM2G	RCP 4.5	1.61	21	21		
HadGEM2-AO	RCP 2.6	1.74	21			
IPSL-CM5A-LR	RCP 2.6	1.74	23	23	23	23
IPSL-CM5A-MR	RCP 2.6	1.6	21	21	21	
MIROC5	RCP 2.6	1.62	21			21
MPI-ESM-LR	RCP 2.6	1.44	23	23	23	23
MPI-ESM-MR	RCP 2.6	1.36	21	21	21	
MRI-CGCM3	RCP 2.6	1.72	21	21	21	21
NorESM1-M	RCP 2.6	1.52	21	21	21	21
NorESM1-ME	RCP 2.6	1.67	21	21	21	

2.0 °C

Model	RCP	2100 GMST (°C)	GMST	Ocean Dynamics	Thermal Expansion	GIC
bcc-csm1-1-m	RCP 4.5	2.13	21	21	21	
CanESM2	RCP 2.6	2.17	23	23	23	23
CESM1-BGC	RCP 4.5	2.24	21	21		
CESM1-CAM5	RCP 2.6	2.13	23			
CSIRO-MK3-6-0	RCP 2.6	2.04	21		21	
FGOALS-G2	RCP 4.5	2.01	23			
GFDL-ESM2M	RCP 4.5	1.84	22	21	21	
GISS-E2-H-CC	RCP 4.5	2.03	21			
GISS-E2-R	RCP 4.5	1.88	23	23	23	23
GISS-E2-R-CC	RCP 4.5	1.87	21	21	21	
HadGEM2-ES	RCP 2.6	1.97	23	23	23	23
inmcm4	RCP 4.5	2.04	21	21	21	21

2.5 °C

Model	RCP	2100 GMST (°C)	GMST	Ocean Dynamics	Thermal Expansion	GIC
CCSM4	RCP 4.5	2.31	23	23	21	21
CNRM-CM5	RCP 4.5	2.56	23	23	23	23
FIO-ESM	RCP 6.0	2.34	21	21		
GFDL-CM3	RCP 2.6	2.57	21	21	21	21
GFDL-ESM2G	RCP 6.0	2.35	21	21	21	
GFDL-ESM2M	RCP 6.0	2.53	21	21	21	
GISS-E2-R	RCP 6.0	2.52	21	21	21	21
IPSL-CM5B-LR	RCP 4.5	2.37	21	21		
MIROC-ESM	RCP 2.6	2.32	21	21	21	21
MIROC-ESM-CHEM	RCP 2.6	2.42	21	21	21	
MIROC5	RCP 4.5	2.38	21		21	21
MPI-ESM-LR	RCP 4.5	2.38	23	23	23	23
MPI-ESM-MR	RCP 4.5	2.39	21	21	21	
MRI-CGCM3	RCP 4.5	2.51	21	21		21
NorESM1-M	RCP 6.0	2.74	21	21	21	23
NorESM1-M	RCP 4.5	2.33	23	23	21	
NorESM1-ME	RCP 4.5	2.44	21	21	21	

21 = to 2100, 22 = to 2200, 23 = to 2300

Table S-3 Global mean sea level projections from a 1.75 °C and a 2.25 °C GMST scenario. All values are cm above 2000 CE baseline. AIS = Antarctic Ice Sheet, GIS = Greenland Ice Sheet; TE = Thermal Expansion; GIC = Glaciers and Ice Caps; LWS = Land-Water Storage.

	1.75°C			2.25°C		
cm	50	17–83	5–95	50	17–83	5–95
2100—Components						
AIS	6	-4–17	-7–34	6	-4–17	-8–33
GIS	7	4–13	3–20	8	4–14	2–22
Ocean	20	11–30	4–37	23	20–27	17–30
GIC	12	8–15	6–17	12	9–16	5–20
LWS	5	3–7	2–8	5	3–7	2–8
Total	51	36–70	26–88	55	42–72	34–89
Projections by year						
2050	25	20–30	17–34	25	21–30	18–34
2070	36	27–45	22–54	37	30–45	26–54
2100	51	36–70	26–88	55	42–72	34–89
2150	73	45–112	30–157	82	53–120	38–163
2200	99	48–167	22–248	111	58–180	30–260

Table S-4: Expected extreme sea level event amplification factors (AF) for the 10-yr event for 2050, 2100, and 2150 under 1.5°C, 2.0°C, and 2.5°C global mean surface temperature stabilization scenarios.

			10-yr Extreme Sea Level Event								
			2050			2100			2150		
Site	Region	Historical Height (m above MHHW)	AF 1.5°C	AF 2.0°C	AF 2.5°C	AF 1.5°C	AF 2.0°C	AF 2.5°C	AF 1.5°C	AF 2.0°C	AF 2.5°C
Buenos Aires	Argentina	2.15	2.1	2.3	2.3	8.0	13.4	13.6	61.1	115.2	96.2
Fort Denison	Australia	0.63	27.7	57.7	48.6	470.8	788.2	874.3	946.0	1325.1	1329.7
Bundaberg	Australia	0.91	15.9	24.2	21.7	238.9	420.6	454.0	736.1	1092.5	1039.3
Brisbane	Australia	0.65	45.1	73.6	63.6	582.1	912.2	954.0	1060.2	1385.7	1354.2
Spring Bay	Australia	0.57	46.9	85.9	98.2	723.2	1095.1	1151.5	1210.9	1494.5	1515.1
Townsville	Australia	1.18	10.7	14.2	13.2	114.7	188.3	220.4	483.5	794.0	734.7
Broome	Australia	2.27	11.2	12.1	13.2	39.7	51.1	56.6	129.5	200.9	176.5
Cocos	Australia	0.51	182.5	246.9	325.7	1323.4	1537.5	1585.9	1609.6	1666.7	1711.9
Darwin	Australia	1.53	18.6	20.3	21.9	90.5	127.8	142.3	334.9	522.9	471.5
Esperance	Australia	0.74	23.2	30.5	39.2	462.5	683.7	788.9	1037.8	1311.7	1328.8
Fremantle	Australia	0.74	22.6	30.4	39.4	479.6	735.1	844.0	1124.7	1370.3	1415.3
Cananeia	Brazil	0.96	19.6	29.3	26.9	427.8	717.4	753.3	1152.6	1349.0	1398.0
Ilha Fiscal, RJ	Brazil	0.83	15.3	23.3	21.1	344.8	619.6	646.5	947.3	1211.0	1222.8
Victoria, BC	Canada	0.91	4.8	6.0	7.1	102.0	135.6	184.3	377.5	601.3	539.0
Prince Rupert	Canada	1.56	4.8	5.3	5.4	39.0	44.4	51.6	157.8	172.5	209.2
Tofino	Canada	1.11	1.7	2.1	2.4	30.9	38.3	51.0	132.3	207.4	179.4
St. John's-A	Canada	0.82	24.0	37.4	42.5	276.7	634.2	647.6	658.2	1063.3	1066.0
Halifax	Canada	0.84	34.4	47.6	57.3	436.8	844.3	921.5	974.3	1275.4	1415.9
Churchill	Canada	1.28	0.1	0.2	0.1	1.7	4.2	3.5	10.5	10.4	10.6
Puerto Montt	Chile	1.60	7.1	8.4	9.2	32.9	47.4	52.1	128.7	229.4	188.7
Juan Fernandez-B	Chile	0.52	33.1	47.1	52.7	595.5	813.2	911.6	1052.3	1291.9	1280.2
Antofagasta	Chile	0.48	20.4	39.5	42.7	463.3	732.9	804.7	888.2	1184.1	1172.0
Easter-C	Chile	0.59	12.0	19.6	19.0	520.7	752.2	821.9	1060.9	1298.9	1288.6
Valparaiso	Chile	0.53	13.7	23.2	24.7	273.0	489.4	545.0	681.4	1004.7	968.6
Xiamen	China	1.43	6.3	7.4	8.7	73.7	99.8	128.1	326.6	525.3	491.7
Buenaventura	Colombia	1.06	22.3	27.5	27.6	199.0	310.5	340.4	655.6	956.3	900.4
Tumaco	Colombia	0.88	10.8	15.9	16.0	125.1	209.6	232.7	413.8	692.5	618.8
Cartagena	Colombia	0.25	1817.7	1743.5	1802.9	1826.0	1819.3	-1000.0	1823.6	1812.5	1824.7
Penrhyn	Cook Islands	0.34	439.3	632.6	616.9	1566.4	1640.3	1682.4	1649.2	1695.5	1728.5
Quepos-A	Costa Rica	0.75	32.6	44.5	46.6	489.0	719.2	795.7	1045.9	1298.7	1291.2
Hornbaek	Denmark	1.25	4.3	42.8	3.9	37.1	282.8	46.7	173.2	343.2	196.4
Gedser	Denmark	1.29	3.8	23.7	3.4	39.8	223.7	51.8	203.4	310.2	242.3
Baltra-B	Ecuador	0.71	19.0	30.1	31.3	482.6	700.2	779.8	1009.7	1264.5	1257.7
Santa Cruz	Ecuador	0.63	35.4	55.9	57.4	670.3	898.2	990.1	1149.2	1369.2	1372.3
La Libertad	Ecuador	0.74	51.4	75.2	75.6	972.4	1178.3	1287.4	1506.1	1606.6	1641.5
Acajutla-A	El Salvador	0.63	56.3	80.0	86.1	842.9	1073.5	1167.9	1331.0	1492.8	1511.3
Chuuk	Fd. St. Micronesia	0.40	205.4	285.8	295.0	1205.4	1415.1	1517.6	1440.3	1578.5	1611.3
Kapingamarangi	Fd. St. Micronesia	0.50	123.9	162.6	189.2	1200.1	1343.8	1462.8	1468.8	1597.7	1616.5
Pohnpei-B	Fd. St. Micronesia	0.51	129.0	173.3	173.7	1127.9	1338.5	1438.0	1440.1	1576.0	1603.1
Yap-B	Fd. St. Micronesia	0.54	72.1	100.0	109.0	969.5	1301.2	1378.5	1394.6	1549.2	1574.5
Suva-C	Fiji	0.51	270.9	329.3	330.8	1572.7	1531.3	1713.4	1737.9	1751.9	1730.9
Noumea	France	0.43	209.7	317.8	287.8	1263.3	1440.7	1565.8	1472.5	1626.4	1585.7

Continued on next page

Table S-4 – continued from previous page

			10-yr Extreme Sea Level Event								
			2050			2100			2150		
Site	Region	Historical Height (m above MHHW)	AF 1.5°C	AF 2.0°C	AF 2.5°C	AF 1.5°C	AF 2.0°C	AF 2.5°C	AF 1.5°C	AF 2.0°C	AF 2.5°C
Brest	France	1.70	8.6	7.9	9.4	37.4	50.0	55.3	138.0	205.9	168.7
Marseille	France	0.68	10.2	124.6	15.3	265.2	577.0	414.5	821.6	766.9	1066.7
Rikitea	French Polynesia	0.31	536.8	775.0	759.1	1587.3	1671.6	1695.4	1641.7	1711.5	1685.0
Papeete-B	French Polynesia	0.31	648.2	916.6	882.1	1680.7	1707.5	1771.0	1715.2	1755.5	1744.2
Cuxhaven	Germany	2.65	2.1	2.1	2.0	5.7	11.9	6.6	35.7	31.6	34.6
Malin Head	Ireland	1.27	4.6	4.9	3.8	32.3	54.3	35.8	135.7	123.1	142.2
Hakodate	Japan	0.48	34.7	57.5	110.6	520.7	766.1	873.8	900.3	1178.0	1152.6
Hamada	Japan	0.63	27.7	43.6	79.4	682.8	941.2	1038.2	1144.7	1399.3	1351.8
Maisaka	Japan	0.77	1.9	2.2	4.6	76.5	124.0	176.4	294.3	521.1	509.4
Ishigaki	Japan	0.78	23.1	33.1	54.2	641.5	825.3	962.1	1153.9	1374.2	1379.8
Naha	Japan	0.71	40.6	59.5	104.2	764.3	954.8	1118.8	1220.7	1418.4	1438.0
Toyama	Japan	0.47	174.6	269.9	415.4	1328.3	1501.1	1532.6	1540.7	1661.5	1621.8
Hosojima	Japan	0.81	6.2	8.5	15.0	202.5	329.1	407.8	594.3	903.0	875.3
Kushiro	Japan	0.52	1579.0	1545.0	1593.1	-1000.0	1823.5	1826.1	1825.8	1822.6	1826.0
Abashiri	Japan	0.64	39.2	82.7	93.0	678.5	949.3	1019.6	1195.3	1370.7	1382.6
Mera	Japan	0.60	156.2	215.3	306.9	1527.8	1626.6	1626.7	1733.9	1753.7	1721.8
Wakkanai	Japan	0.53	125.6	222.2	305.7	1285.6	1513.1	1499.4	1580.3	1686.0	1651.0
Chichijima	Japan	0.57	108.2	237.9	313.6	1216.7	1330.7	1499.3	1539.1	1614.7	1633.1
Nishinoomote	Japan	0.71	38.9	53.6	91.2	725.8	946.0	1049.7	1213.0	1444.9	1419.5
Naze	Japan	0.73	63.6	81.3	137.8	967.2	1132.1	1297.9	1385.3	1545.7	1556.7
Hachinohe	Japan	0.50	398.3	523.2	671.5	1662.6	1745.5	1736.4	1780.5	1786.6	1780.5
Miyakejima	Japan	0.87	157.5	177.6	240.6	1670.3	1718.3	1709.8	1816.2	1810.4	1806.0
Nakano Shima	Japan	0.74	51.6	67.9	112.8	876.8	1057.0	1165.0	1322.2	1511.0	1484.3
Ofunato	Japan	0.50	1232.5	1393.7	1308.6	1825.4	1823.5	1821.2	1825.2	1823.3	1823.9
Nagasaki	Japan	0.83	29.9	37.8	50.1	410.3	597.2	685.3	896.2	1194.2	1152.1
Aburatsu	Japan	0.82	10.3	14.3	25.9	355.7	541.5	643.9	883.1	1191.3	1160.9
Kushimoto	Japan	0.68	85.8	115.6	180.6	1277.4	1462.0	1484.3	1626.6	1696.3	1679.0
Cendering	Malaysia	0.90	13.9	17.5	19.4	239.8	372.4	439.0	672.2	935.3	893.0
Johor Baharu	Malaysia	0.81	34.6	42.2	46.9	439.9	616.4	716.2	922.4	1169.9	1147.1
Kuantan	Malaysia	0.96	18.6	22.5	24.5	260.4	392.1	461.9	724.9	985.7	946.7
Keling	Malaysia	0.65	41.0	51.7	58.7	527.6	711.7	820.4	942.2	1174.8	1152.2
Lumut	Malaysia	0.76	26.3	34.8	41.2	413.3	590.0	670.4	855.0	1111.8	1073.0
Kelang	Malaysia	1.22	12.7	14.2	15.7	117.4	168.9	202.6	436.8	635.8	581.3
Langkawi	Malaysia	0.83	29.4	37.1	42.9	329.0	484.6	556.4	756.5	1018.9	973.8
Penang	Malaysia	0.72	47.6	61.8	72.9	543.7	745.8	830.2	978.3	1219.8	1191.9
Port Louis-C	Mauritius	0.41	110.9	186.7	267.1	1061.5	1358.7	1386.4	1347.1	1548.3	1560.3
Rodrigues	Mauritius	0.69	28.4	42.9	56.6	716.2	963.6	1056.8	1257.7	1485.4	1482.3
Manzanillo-A	Mexico	0.52	262.5	386.6	401.8	1681.3	1697.5	1745.6	1784.1	1765.7	1786.4
Ensenada	Mexico	0.65	54.1	79.5	84.0	708.0	956.1	1034.1	1255.2	1415.0	1441.5
Salina Cruz	Mexico	0.53	127.6	187.8	194.5	1333.6	1477.6	1566.4	1598.8	1665.2	1688.8
Acapulco-A, Gro.	Mexico	0.51	440.5	609.7	642.6	1806.2	1787.8	1811.9	1820.6	1804.4	1816.3
Cabo San Lucas	Mexico	0.59	49.7	75.0	76.3	738.5	984.4	1059.2	1222.9	1405.8	1419.9
Guaymas	Mexico	0.52	181.9	263.2	343.3	1591.7	1648.7	1674.6	1753.3	1748.7	1771.2
Saipan-B	N. Mariana Islands	0.44	126.9	196.7	205.8	1209.2	1335.7	1494.0	1419.4	1537.1	1598.0
Marsden Point	New Zealand	0.75	8.3	28.9	22.0	343.3	689.4	714.2	886.6	1297.5	1256.3
Tauranga	New Zealand	0.51	62.7	207.0	154.5	966.7	1337.0	1409.6	1300.7	1607.6	1611.8

Continued on next page

Table S-4 – continued from previous page

			10-yr Extreme Sea Level Event								
			2050			2100			2150		
Site	Region	Historical Height (m above MHHW)	AF 1.5°C	AF 2.0°C	AF 2.5°C	AF 1.5°C	AF 2.0°C	AF 2.5°C	AF 1.5°C	AF 2.0°C	AF 2.5°C
Taranaki	New Zealand	1.10	3.8	7.9	6.5	91.2	209.7	212.8	454.4	813.3	730.8
Wellington	New Zealand	0.49	141.6	383.0	291.0	1333.1	1581.7	1639.4	1538.0	1727.0	1742.3
Tregde	Norway	0.77	11.2	17.3	10.2	111.6	209.4	147.1	350.2	403.1	453.7
Rorvik	Norway	1.15	1.5	3.1	1.7	17.0	33.9	23.3	75.6	79.1	79.3
Ny-Alesund	Norway	0.66	0.3	18.0	0.0	5.4	18.0	5.0	50.3	19.8	31.0
Vardo	Norway	1.03	3.6	14.5	5.8	37.1	108.6	66.0	133.6	224.5	190.6
Balboa	Panama	1.24	17.2	19.1	20.3	109.3	177.8	189.9	423.7	706.7	650.9
Cristobal	Panama	0.29	926.7	959.1	1112.7	1658.3	1717.6	1793.7	1655.2	1727.0	1760.7
Rabaul	Papua New Guinea	0.36	296.9	387.6	441.3	1378.2	1488.8	1612.2	1529.1	1639.5	1662.1
Lobos de Afuera	Peru	0.60	22.6	42.6	42.3	627.6	858.4	941.6	1087.6	1319.6	1318.2
Callao-B	Peru	0.46	29.5	58.4	66.2	703.9	932.2	1034.4	1084.7	1322.3	1325.0
Legaspi	Philippines	0.51	291.3	431.2	460.3	1630.6	1679.5	1748.6	1753.0	1746.9	1788.1
Manila	Philippines	0.69	428.3	561.7	610.5	1823.1	1817.2	1824.9	1825.2	1820.2	1825.8
Cascais	Portugal	0.93	17.2	15.3	21.9	158.6	240.3	314.2	562.7	808.0	811.6
Funchal-B	Portugal	0.64	94.1	85.8	129.7	748.3	951.0	1063.9	1193.4	1369.9	1481.8
Kanton-B	Rep. of Kiribati	0.43	123.8	200.3	198.1	1204.7	1379.0	1418.8	1430.8	1561.0	1592.8
Christmas-B	Rep. of Kiribati	0.42	210.8	334.7	328.4	1423.0	1513.3	1554.2	1560.1	1641.8	1671.7
Majuro-A	Rep. of Marshall I	0.60	111.1	143.0	137.0	1039.2	1243.9	1343.9	1420.2	1562.5	1592.8
Kwajalein	Rep. of Marshall I	0.51	225.0	283.7	281.9	1296.7	1483.9	1557.4	1551.9	1633.8	1682.8
Malakal-B	Republic of Belau	0.51	140.7	183.8	198.0	1087.0	1407.5	1461.0	1468.3	1607.0	1629.5
Kaohsiung	Republic of China	0.58	26.6	40.5	54.0	488.4	668.6	780.4	842.9	1096.1	1073.1
Keelung	Republic of China	0.68	22.4	34.9	60.2	765.3	964.3	1067.9	1184.8	1401.1	1384.4
Luderitz	South Africa	0.55	88.6	112.0	130.8	1019.1	1269.9	1382.3	1374.7	1549.3	1596.3
Saldahna Bay	South Africa	0.60	80.5	96.6	112.9	846.0	1114.4	1193.7	1259.5	1471.4	1502.8
Simon's Town	South Africa	0.62	76.4	93.1	111.0	956.5	1230.9	1318.9	1396.4	1568.7	1606.7
Port Nolloth	South Africa	0.64	59.0	72.3	75.7	769.0	1050.7	1150.0	1252.8	1476.8	1518.1
Port Elizabeth	South Africa	0.76	25.2	34.6	36.2	426.6	665.8	751.1	946.3	1260.0	1257.4
La Coruna	Spain	1.07	23.4	21.0	25.5	158.8	224.2	267.1	562.4	757.0	766.0
Ceuta	Spain	0.45	49.8	74.0	105.3	642.0	808.4	1011.2	1074.0	1282.3	1362.4
Vigo	Spain	1.10	17.6	16.2	20.5	145.7	211.4	257.9	547.2	758.8	755.6
Stockholm	Sweden	0.76	2.8	231.0	1.6	30.6	462.3	34.6	84.5	12.1	105.0
Goteborg-Torsh.	Sweden	1.12	2.9	14.8	2.5	28.6	158.5	34.3	126.4	183.5	133.7
Zanzibar	Tanzania	1.06	30.5	35.6	37.5	206.1	307.3	360.8	592.4	887.7	855.6
Ko Lak	Thailand	0.93	30.5	37.0	40.0	422.1	601.7	688.6	974.6	1215.5	1194.8
Stornoway	United Kingdom	1.39	6.9	6.4	6.1	35.4	47.2	39.3	141.3	116.2	144.3
Lerwick	United Kingdom	0.84	9.6	12.1	8.4	89.3	128.8	103.2	284.4	270.6	332.7
Faraday	United Kingdom	0.80	4.8	7.6	5.0	42.4	69.7	74.5	299.9	606.7	534.0
Gibraltar-A	United Kingdom	0.43	49.4	70.0	100.2	515.3	688.7	876.6	916.6	1160.0	1230.1
Bermuda-B	United Kingdom	0.53	72.6	92.1	120.9	943.6	1092.6	1163.3	1325.0	1471.5	1453.0
Newlyn, Cornwall	United Kingdom	1.24	15.8	15.8	15.5	86.5	126.6	112.5	305.7	373.4	412.4
Seward-C, AK	USA	1.28	0.5	0.7	0.6	8.9	11.3	10.6	51.1	59.4	61.7
Ketchikan, AK	USA	1.53	2.5	2.7	2.8	22.3	25.7	30.0	95.9	102.1	124.1
Valdez, AK	USA	1.29	0.2	0.4	0.3	5.8	7.3	6.7	34.9	41.4	41.2
Yakutat, AK	USA	1.26	0.0	0.0	0.0	2.9	3.4	3.3	16.3	15.1	17.2
Seldovia, AK	USA	1.79	0.1	0.1	0.1	0.8	0.8	0.8	10.2	10.2	9.9
Sitka, AK	USA	1.21	1.0	1.1	1.2	17.2	19.9	23.2	78.6	80.0	98.9

Continued on next page

Table S-4 – continued from previous page

			10-yr Extreme Sea Level Event								
			2050			2100			2150		
Site	Region	Historical Height (m above MHHW)	AF 1.5°C	AF 2.0°C	AF 2.5°C	AF 1.5°C	AF 2.0°C	AF 2.5°C	AF 1.5°C	AF 2.0°C	AF 2.5°C
Sand Point, AK	USA	1.12	5.1	5.5	6.2	81.9	97.1	128.9	344.9	400.7	491.3
Dutch Harbor-B, AK	USA	0.72	0.9	1.0	1.4	40.9	50.6	65.5	142.5	170.3	200.2
Cordova-B, AK	USA	1.35	7.7	10.0	9.4	90.3	117.5	119.7	422.3	460.4	523.7
Kodiak Isl., AK	USA	1.09	0.1	0.1	0.2	3.8	4.2	4.4	20.1	19.1	21.8
Adak, AK	USA	0.78	4.9	6.0	6.8	93.3	127.8	159.5	288.1	344.8	408.0
San Francisco, CA	USA	0.68	21.0	33.8	37.4	536.3	764.8	866.7	1127.2	1328.1	1340.7
San Diego, CA	USA	0.68	57.1	81.3	86.5	694.9	943.9	1020.7	1273.8	1428.0	1456.9
Los Angeles, CA	USA	0.66	32.3	49.8	52.4	418.9	633.1	714.8	928.3	1176.4	1176.5
Crescent City, CA	USA	0.92	2.9	3.8	4.5	65.3	85.0	125.3	258.3	426.0	376.1
Monterey, CA	USA	0.68	22.1	34.5	39.3	448.7	664.4	758.5	996.7	1230.4	1231.6
Port San Luis, CA	USA	0.69	16.9	27.6	31.2	325.4	500.2	595.0	814.2	1082.7	1070.9
Santa Monica, CA	USA	0.70	28.7	44.2	46.9	433.3	647.8	730.6	979.0	1213.3	1216.9
La Jolla, CA	USA	0.66	56.6	82.9	88.7	727.3	980.2	1055.3	1292.6	1441.4	1471.5
New London, CT	USA	1.04	5.7	7.7	8.5	140.4	327.4	338.6	544.7	944.0	970.9
Fernandina Beach, FL	USA	0.92	13.2	14.6	18.8	242.1	472.2	508.8	814.1	1119.1	1178.7
St. Petersburg, FL	USA	0.79	9.7	22.4	15.5	438.8	764.6	842.8	1111.3	1339.7	1405.1
Pensacola, FL	USA	0.84	4.2	9.9	6.3	223.8	490.0	498.3	815.7	1137.3	1149.4
Mayport, FL	USA	0.61	72.1	79.0	109.7	820.6	1158.2	1266.2	1315.5	1480.0	1608.8
Limetree Bay, FL	USA	0.30	705.7	672.1	832.3	1648.3	1633.8	1737.2	1653.5	1684.7	1743.2
Key West, FL	USA	0.43	279.3	331.7	436.7	1485.9	1532.5	1700.7	1631.4	1665.2	1723.4
Fort Pulaski, GA	USA	0.76	53.8	57.0	77.4	674.3	1022.1	1114.9	1301.2	1477.0	1605.1
Hilo, HI	USA	0.42	506.3	612.4	720.9	1698.8	1724.1	1749.2	1744.2	1764.9	1760.6
French Frigate, HI	USA	0.38	363.7	541.1	572.1	1486.5	1621.3	1668.2	1568.8	1668.6	1666.3
Kahului, HI	USA	0.36	657.1	764.4	876.1	1691.7	1716.7	1746.6	1718.6	1751.9	1745.7
Mokuoloe, HI	USA	0.36	452.6	558.3	657.9	1586.5	1645.7	1687.7	1629.9	1707.0	1699.2
Honolulu-B, HI	USA	0.36	446.1	552.1	650.8	1585.0	1644.6	1687.0	1629.0	1706.5	1698.8
Nawiliwili, HI	USA	0.37	364.0	470.9	548.9	1507.4	1607.7	1641.6	1575.6	1678.1	1669.9
Grand Isle, LA	USA	1.03	17.7	35.9	27.8	1595.4	1635.1	1760.0	1823.8	1802.7	1824.2
Woods Hole, MA	USA	0.92	12.9	17.9	20.2	261.7	574.5	606.6	786.9	1127.8	1241.6
Nantucket, MA	USA	0.95	8.7	13.3	14.3	263.8	569.1	610.2	844.7	1165.3	1294.9
Boston, MA	USA	1.04	15.2	18.8	22.4	189.4	390.8	417.5	587.2	960.3	987.7
Portland, ME	USA	0.93	19.5	25.9	29.6	196.0	418.1	436.0	532.8	919.2	918.2
Eastport, ME	USA	1.27	18.8	23.2	26.7	111.7	234.6	231.8	325.1	671.6	539.7
Duck Pier, NC	USA	0.90	24.0	34.8	43.9	463.4	860.3	914.0	1181.7	1392.4	1538.1
Wilmington, NC	USA	0.58	47.2	97.5	104.3	811.2	1194.8	1279.5	1309.9	1482.1	1632.3
Atlantic City, NJ	USA	0.94	24.4	34.7	43.3	450.6	844.7	916.6	1156.3	1382.4	1562.9
Cape May, NJ	USA	0.88	26.5	33.7	43.5	468.6	893.6	961.6	1175.2	1390.4	1596.1
Montauk, NY	USA	0.94	12.8	18.1	20.7	270.9	573.5	624.9	844.6	1172.9	1308.4
New York, NY	USA	1.09	6.1	8.4	9.8	154.4	358.9	367.3	587.6	985.0	1028.1
Charleston, OR	USA	0.96	6.7	8.2	9.8	126.3	168.5	237.2	472.4	709.8	658.3
South Beach, OR	USA	1.04	9.0	10.8	12.2	156.2	205.8	280.0	587.4	841.8	793.0
Astoria, OR	USA	1.00	3.3	4.2	4.8	59.4	75.1	107.7	237.0	389.7	336.2
Newport, RI	USA	0.85	24.0	32.1	38.6	360.7	710.3	785.9	921.0	1215.9	1361.3
Charleston, SC	USA	0.77	36.0	43.7	55.3	585.8	939.9	1028.5	1234.7	1444.6	1560.0
Galveston (Pier 21), TX	USA	0.98	14.3	30.3	21.6	945.3	1245.9	1382.6	1693.6	1696.9	1770.8
Rockport, TX	USA	0.63	142.5	242.5	247.1	1677.4	1705.0	1775.4	1801.9	1779.1	1817.4

Continued on next page

Table S-4 – continued from previous page

			10-yr Extreme Sea Level Event								
			2050			2100			2150		
Site	Region	Historical Height (m above MHHW)	AF 1.5°C	AF 2.0°C	AF 2.5°C	AF 1.5°C	AF 2.0°C	AF 2.5°C	AF 1.5°C	AF 2.0°C	AF 2.5°C
Port Isabel, TX	USA	0.64	40.7	80.2	74.0	1083.4	1337.4	1479.5	1537.6	1627.7	1707.2
Galveston (P. Pier), TX	USA	1.14	8.3	15.5	11.1	553.6	898.1	990.4	1532.0	1607.4	1695.5
Chesapeake BBT, VA	USA	1.05	12.1	16.0	19.7	290.8	615.0	656.6	1019.0	1287.5	1432.0
Neah Bay, WA	USA	1.11	1.3	1.7	2.0	25.2	31.2	42.4	108.2	169.5	143.3
Willapa Bay, WA	USA	1.38	2.6	3.0	3.3	34.1	41.5	56.6	167.5	266.6	230.5
Lewes, DE	USA	1.04	10.6	13.2	16.8	228.8	546.6	553.9	836.9	1172.4	1305.8
Apra Harbor, Guam	USA Trust	0.29	865.1	948.3	1123.5	1635.8	1662.1	1765.1	1697.8	1708.4	1758.5
Wake	USA Trust	0.52	107.9	214.0	178.2	1203.1	1374.8	1488.5	1453.3	1574.0	1607.5
Johnston	USA Trust	0.54	59.4	102.4	90.4	982.1	1212.5	1258.2	1300.0	1491.9	1504.7
Midway	USA Trust	0.61	24.4	59.8	66.5	775.1	1011.4	1192.0	1216.1	1406.4	1433.4
Pago Pago	USA Trust	0.38	585.3	747.5	777.7	1723.7	1761.1	1774.8	1758.3	1777.1	1781.8
Charlotte Amalie, VI	USA Trust	0.31	627.4	602.4	744.1	1611.9	1600.1	1720.4	1638.5	1672.8	1737.1
San Juan, PR	USA Trust	0.33	583.3	561.2	703.8	1602.7	1595.4	1721.3	1646.4	1680.3	1742.5
Magueyes Island, PR	USA Trust	0.27	955.6	862.7	1050.2	1689.4	1649.7	1759.5	1674.0	1695.9	1750.5

Table S-5: Expected extreme sea level event amplification factors (AF) for the 100-yr event for 2050, 2100, and 2150 under 1.5°C, 2.0°C, and 2.5°C global mean surface temperature stabilization scenarios.

			100-yr Extreme Sea Level Event								
			2050			2100			2150		
Site	Region	Historical Height (m above MHHW)	AF 1.5°C	AF 2.0°C	AF 2.5°C	AF 1.5°C	AF 2.0°C	AF 2.5°C	AF 1.5°C	AF 2.0°C	AF 2.5°C
Buenos Aires	Argentina	3.07	1.6	1.7	1.7	3.7	5.4	5.6	93.2	162.8	130.1
Fort Denison	Australia	0.74	74.0	191.3	154.8	2604.8	4878.1	5520.6	7389.2	11399.7	11338.3
Bundaberg	Australia	1.24	6.3	10.9	9.3	526.1	953.9	1068.3	3298.1	6105.6	5416.5
Brisbane	Australia	0.78	103.2	204.3	169.4	3055.4	5531.9	5788.3	8173.7	11886.5	11375.0
Spring Bay	Australia	0.70	93.5	211.0	253.5	3651.9	7156.2	7339.8	9453.0	13012.9	12930.9
Townsville	Australia	1.35	28.2	43.1	38.4	577.4	938.8	1116.8	3198.8	5678.8	5091.7
Broome	Australia	2.41	40.6	47.9	53.4	271.3	361.5	404.3	1002.3	1563.0	1367.0
Cocos	Australia	0.58	859.7	1155.5	1678.5	11109.0	13704.8	14419.1	15158.6	16139.3	16551.0
Darwin	Australia	1.69	43.4	57.3	64.3	540.6	775.5	875.0	2370.7	3842.3	3392.5
Esperance	Australia	0.81	123.3	160.7	211.8	3277.4	5100.9	6069.6	9037.4	12064.1	12018.5
Fremantle	Australia	0.89	46.6	67.3	93.5	2245.7	3852.2	4583.5	8092.4	11368.5	11292.6
Cananeia	Brazil	1.37	6.4	9.3	8.4	592.9	1353.7	1259.0	4849.6	8088.6	7297.4
Ilha Fiscal, RJ	Brazil	1.06	16.1	26.5	23.1	1065.3	2403.5	2295.6	5760.9	8950.6	8395.6
Victoria, BC	Canada	1.06	10.5	14.3	17.9	544.7	696.1	976.1	2545.8	4176.8	3627.4
Prince Rupert	Canada	1.74	10.7	12.0	12.7	207.8	241.4	277.9	1071.5	1155.3	1390.4
Tofino	Canada	1.29	2.6	3.6	4.6	177.5	208.9	277.5	902.3	1364.6	1170.6
St. John's-A	Canada	1.02	36.3	65.6	73.7	1146.3	3005.4	2957.9	3805.7	8021.2	6721.4
Halifax	Canada	1.16	20.4	30.5	35.9	1079.5	2925.2	2650.4	4398.5	8612.5	7905.3
Churchill	Canada	1.63	0.2	0.2	0.2	2.3	18.4	9.1	68.6	74.5	67.2
Puerto Montt	Chile	1.70	22.3	29.6	34.0	211.4	324.5	359.9	1013.0	1841.2	1492.8
Juan Fernandez-B	Chile	0.61	92.1	148.9	175.7	3706.6	5693.9	6558.9	8825.6	11605.1	11320.1
Antofagasta	Chile	0.60	29.4	75.4	90.8	2288.6	4205.7	4703.6	6657.6	9917.6	9530.2
Easter-C	Chile	0.92	4.1	5.4	5.4	899.1	1586.8	1820.6	5351.6	8024.5	7885.1
Valparaiso	Chile	0.61	36.9	76.0	80.8	1676.3	3310.7	3642.1	5514.9	8763.6	8252.6
Xiamen	China	1.72	8.7	10.9	13.4	257.1	337.8	467.6	1683.2	2916.9	2664.4
Buenaventura	Colombia	1.20	57.7	90.3	89.2	1122.0	1809.4	1982.5	4740.9	7598.9	6859.2
Tumaco	Colombia	1.01	19.6	38.4	38.1	701.6	1194.3	1331.7	2989.0	5320.8	4569.7
Cartagena	Colombia	0.30	17448.6	16125.4	17221.3	18246.5	18141.0	18259.2	18212.7	18077.2	18236.8
Penrhyn	Cook Islands	0.53	243.1	482.3	382.8	9865.1	11895.6	12750.0	13837.9	15372.5	15618.2
Quepos-A	Costa Rica	0.79	231.4	316.5	336.2	4059.5	6204.2	6889.6	9729.8	12414.2	12282.1
Hornbaek	Denmark	1.50	8.1	203.6	7.1	165.9	1894.8	201.3	1004.0	2614.1	1036.9
Gedser	Denmark	1.72	4.1	56.4	3.7	107.2	897.1	131.0	804.1	1645.3	812.7
Baltra-B	Ecuador	0.80	77.6	127.0	135.4	3142.9	4942.8	5561.4	8472.5	11362.3	11149.8
Santa Cruz	Ecuador	0.70	166.7	277.5	287.5	4932.3	7131.0	7926.5	10200.4	12711.2	12656.5
La Libertad	Ecuador	0.85	187.1	288.7	292.7	6316.8	8715.8	9579.3	13210.6	14944.3	15160.8
Acajutla-A	El Salvador	0.71	252.7	372.7	405.2	6062.1	8483.7	9272.9	11865.2	13911.8	14018.1
Chuuk	Fd. St. Micronesia	0.63	97.3	157.9	137.6	5183.1	8454.7	9141.5	10646.7	13057.0	13103.9
Kapingamarangi	Fd. St. Micronesia	0.60	373.8	507.3	602.1	8792.8	10959.8	12016.7	13174.0	14940.5	15107.2
Pohnpei-B	Fd. St. Micronesia	0.63	333.1	462.0	448.6	7488.3	10358.5	11254.9	12536.3	14476.9	14675.7
Yap-B	Fd. St. Micronesia	1.21	1.9	2.0	2.1	586.5	1145.0	1364.5	4044.6	6760.3	5935.7
Suva-C	Fiji	0.63	678.9	868.0	869.2	12607.7	12920.8	15129.7	16207.3	16844.2	16506.5
Noumea	France	0.50	900.0	1363.9	1236.8	10287.9	12596.1	14045.3	13559.6	15589.9	15116.7

Continued on next page

Table S-5 – continued from previous page

			100-yr Extreme Sea Level Event								
			2050			2100			2150		
Site	Region	Historical Height (m above MHHW)	AF 1.5°C	AF 2.0°C	AF 2.5°C	AF 1.5°C	AF 2.0°C	AF 2.5°C	AF 1.5°C	AF 2.0°C	AF 2.5°C
Brest	France	1.82	35.8	31.2	41.0	247.0	339.8	379.9	1073.0	1606.4	1291.4
Marseille	France	0.87	15.6	499.1	21.9	963.6	4145.0	1460.6	4930.7	6820.1	6975.8
Rikitea	French Polynesia	0.32	4712.8	7036.3	6838.5	15635.6	16568.3	16822.7	16299.8	17052.3	16780.3
Papeete-B	French Polynesia	0.56	100.6	229.7	233.9	9406.1	11718.3	12709.0	13945.7	15788.6	15359.6
Cuxhaven	Germany	3.49	2.1	2.2	2.0	5.8	15.8	6.8	114.0	98.8	91.7
Malin Head	Ireland	1.51	6.2	7.5	4.8	146.0	259.0	149.3	834.5	714.2	814.2
Hakodate	Japan	0.56	124.7	212.7	483.1	3504.0	5433.7	6676.3	7586.2	10482.4	10284.0
Hamada	Japan	0.93	8.7	13.5	37.4	1646.5	2769.6	3625.9	6302.3	9466.9	9094.8
Maisaka	Japan	1.44	1.3	1.3	1.4	83.4	102.0	170.5	654.0	1142.1	1089.7
Ishigaki	Japan	0.95	47.5	67.4	125.5	3146.3	4417.8	5659.9	8684.9	11469.8	11371.3
Naha	Japan	0.94	34.4	58.2	136.5	2882.1	4289.6	5742.2	8311.4	11152.9	11122.4
Toyama	Japan	0.61	289.2	510.3	1073.4	8725.1	11292.5	12084.5	13182.1	15232.8	14815.5
Hosojima	Japan	1.16	3.6	4.6	6.9	444.6	680.8	970.1	2551.5	4586.3	4390.5
Kushiro	Japan	0.67	5794.2	7806.7	8727.3	18249.2	18141.0	18246.2	18254.7	18187.4	18257.1
Abashiri	Japan	0.76	106.3	257.6	305.9	3990.0	6277.6	7081.7	9778.1	12027.7	12014.4
Mera	Japan	0.88	59.5	81.1	187.1	6710.4	9446.0	9882.6	13660.3	15424.3	15021.8
Wakkanai	Japan	0.75	81.0	179.7	346.0	6138.0	8598.3	9504.2	12313.8	14541.3	14177.1
Chichijima	Japan	0.85	37.4	144.3	217.8	5522.3	6999.2	8797.9	11175.9	13295.7	13330.3
Nishinoomote	Japan	0.89	58.1	88.0	184.6	3349.2	5107.9	6143.5	8945.4	11963.2	11710.9
Naze	Japan	0.99	46.4	63.4	147.4	3566.4	5150.6	6511.0	9414.2	12279.4	12223.2
Hachinohe	Japan	0.66	655.2	930.3	1692.5	12772.6	14909.2	15083.0	16516.2	17143.2	17010.1
Miyakejima	Japan	1.23	82.4	95.0	157.4	7651.5	9620.7	10135.0	15843.7	16803.4	16646.2
Nakano Shima	Japan	1.08	14.2	20.8	50.9	2291.0	3321.0	4209.1	7719.0	10715.1	10412.7
Ofunato	Japan	0.63	4012.1	5546.4	6786.9	18087.5	18116.8	17984.8	18249.9	18208.7	18194.9
Nagasaki	Japan	0.96	92.1	127.2	179.0	2368.8	3643.6	4383.9	6959.2	10046.9	9644.7
Aburatsu	Japan	1.17	6.0	7.6	12.8	711.4	1141.7	1598.4	3986.1	6779.7	6545.3
Kushimoto	Japan	0.82	211.7	290.5	501.0	8264.0	10860.2	11482.0	14305.0	15834.8	15613.1
Cendering	Malaysia	1.10	20.9	28.4	32.7	1016.8	1722.8	2076.8	4495.4	6912.7	6352.5
Johor Baharu	Malaysia	0.93	116.5	150.9	171.5	2722.3	4082.5	4861.6	7522.7	10139.1	9806.0
Kuantan	Malaysia	1.13	40.1	52.9	60.0	1280.7	2077.7	2495.5	5208.2	7720.5	7197.4
Keling	Malaysia	0.74	163.3	214.1	250.4	3674.0	5245.1	6217.4	8138.4	10580.8	10275.8
Lumut	Malaysia	0.84	125.6	171.6	205.3	3002.7	4456.4	5177.0	7454.1	10068.4	9612.1
Kelang	Malaysia	1.32	57.8	68.5	77.6	809.6	1170.3	1419.0	3564.4	5328.1	4805.6
Langkawi	Malaysia	0.91	147.1	196.2	231.5	2397.4	3670.2	4253.1	6543.7	9150.8	8644.4
Penang	Malaysia	0.84	154.4	215.4	265.7	3437.1	5047.9	5803.2	8080.7	10670.0	10272.3
Port Louis-C	Mauritius	0.46	555.7	987.8	1560.5	8921.9	12104.4	12529.9	12577.9	14901.7	14981.5
Rodrigues	Mauritius	1.02	8.7	13.5	20.6	1687.2	2708.0	3170.0	6926.6	10088.0	9699.1
Manzanillo-A	Mexico	0.63	687.6	1131.0	1152.8	14202.6	15225.6	15919.7	17117.3	17153.7	17414.7
Ensenada	Mexico	0.70	341.0	513.3	542.2	5695.5	8084.2	8906.9	11591.2	13455.7	13647.4
Salina Cruz	Mexico	0.69	192.5	303.7	319.9	7776.2	10389.8	11292.8	13540.1	15174.6	15334.6
Acapulco-A, Gro.	Mexico	0.71	289.9	515.0	534.9	14774.2	15587.9	16308.8	17667.0	17511.8	17745.7
Cabo San Lucas	Mexico	0.63	331.4	505.2	513.5	6270.5	8715.7	9446.7	11511.8	13503.1	13612.9
Guaymas	Mexico	0.63	487.6	770.5	1047.9	12568.5	14063.9	14570.1	16479.3	16833.4	17094.3
Saipan-B	N. Mariana Islands	1.33	1.4	1.5	1.5	320.4	685.7	572.0	2348.8	4299.9	3898.1
Marsden Point	New Zealand	1.96	1.3	1.4	1.4	38.1	59.2	56.6	514.6	884.4	672.5
Tauranga	New Zealand	0.58	259.1	945.8	699.5	7152.6	11289.1	11974.3	11707.8	15271.6	15172.6

Continued on next page

Table S-5 – continued from previous page

			100-yr Extreme Sea Level Event								
			2050			2100			2150		
Site	Region	Historical Height (m above MHHW)	AF 1.5°C	AF 2.0°C	AF 2.5°C	AF 1.5°C	AF 2.0°C	AF 2.5°C	AF 1.5°C	AF 2.0°C	AF 2.5°C
Taranaki	New Zealand	2.14	1.4	1.6	1.5	28.4	49.4	45.4	396.0	672.6	535.1
Wellington	New Zealand	0.59	404.3	1349.2	960.9	9394.2	13290.1	13890.4	13673.7	16508.4	16557.0
Tregde	Norway	0.99	12.3	31.9	11.1	439.5	881.5	552.7	2013.6	2143.8	2349.0
Rorvik	Norway	1.72	1.2	1.6	1.2	38.1	82.5	48.1	282.8	255.6	274.4
Ny-Alesund	Norway	0.76	0.9	138.4	0.1	42.8	152.4	40.9	444.1	173.1	271.3
Vardo	Norway	1.24	5.2	45.5	10.0	175.8	552.5	309.2	826.1	1338.5	1112.6
Balboa	Panama	1.33	86.0	103.7	110.5	779.9	1276.7	1357.9	3436.9	5928.1	5358.9
Cristobal	Panama	0.35	4136.4	5255.5	6261.8	14958.3	16320.8	17375.8	15734.3	16886.0	17235.9
Rabaul	Papua New Guinea	0.38	2225.3	3019.3	3441.1	13149.1	14461.5	15735.5	15010.5	16217.4	16430.6
Lobos de Afuera	Peru	0.68	89.8	179.4	178.6	4354.6	6513.4	7179.7	9440.5	12080.3	11952.9
Callao-B	Peru	0.62	30.9	74.7	88.5	3117.0	5013.0	5631.1	7807.3	10824.3	10596.9
Legaspi	Philippines	0.64	695.7	1148.9	1216.6	12559.7	14416.6	15575.8	16237.7	16739.9	17228.3
Manila	Philippines	0.84	1101.4	1544.5	1699.1	17449.7	17639.5	18002.5	18242.6	18122.2	18238.0
Cascais	Portugal	1.04	65.8	57.0	90.4	954.5	1496.1	1990.7	4219.3	6431.6	6265.3
Funchal-B	Portugal	0.68	669.3	609.9	937.4	6345.1	8371.8	9545.3	11209.6	13138.5	14226.4
Kanton-B	Rep. of Kiribati	0.55	244.9	407.8	425.0	7969.8	10387.5	10773.3	12322.9	14266.8	14497.6
Christmas-B	Rep. of Kiribati	0.48	924.8	1618.7	1555.5	12459.3	13772.5	14252.7	14788.1	15910.8	16184.2
Majuro-A	Rep. of Marshall I	0.63	846.8	1094.9	1040.5	9454.3	11645.9	12657.3	13756.1	15316.8	15610.8
Kwajalein	Rep. of Marshall I	0.54	1681.4	2158.0	2104.2	12072.9	14150.8	14953.3	15114.8	16082.5	16575.4
Malakal-B	Republic of Belau	0.54	1010.6	1328.6	1437.1	9968.8	13338.5	13942.3	14234.0	15786.3	15977.2
Kaohsiung	Republic of China	0.80	15.8	28.5	42.1	1896.3	2910.3	3628.1	5528.1	8076.3	7746.9
Keelung	Republic of China	1.05	6.7	9.0	13.8	1673.2	2675.4	3263.9	6483.3	9206.4	8949.6
Luderitz	South Africa	0.61	465.1	598.6	699.4	8104.4	10835.7	11996.9	12683.8	14818.0	15266.0
Saldahna Bay	South Africa	0.62	666.7	803.3	940.2	7818.7	10537.3	11339.6	12230.9	14472.8	14760.1
Simon's Town	South Africa	0.72	275.9	350.8	425.1	6300.0	9155.1	10073.1	12080.2	14525.0	14828.7
Port Nolloth	South Africa	0.69	359.9	450.1	471.1	6171.3	8938.2	9864.1	11570.5	14122.4	14477.1
Port Elizabeth	South Africa	0.87	85.8	124.4	130.7	2510.9	4193.4	4884.3	7563.9	10960.4	10722.2
La Coruna	Spain	1.17	112.6	97.1	126.3	1052.5	1510.2	1824.3	4424.9	6156.5	6095.7
Ceuta	Spain	0.54	147.6	274.8	383.6	3750.3	5484.9	7093.5	8753.4	11262.0	11932.3
Vigo	Spain	1.37	15.9	14.2	21.1	471.4	712.6	894.5	2790.8	4155.2	3842.7
Stockholm	Sweden	0.98	3.1	1612.2	1.7	159.2	3792.2	170.4	535.7	95.1	633.5
Goteborg-Torsh.	Sweden	1.43	3.3	43.9	2.8	111.7	758.8	126.4	678.4	1041.6	647.0
Zanzibar	Tanzania	1.11	224.1	264.9	281.4	1695.1	2551.4	3026.0	5297.3	8180.1	7828.1
Ko Lak	Thailand	1.05	119.3	151.1	165.6	2644.5	4022.4	4702.8	8015.3	10618.9	10290.9
Stornoway	United Kingdom	1.50	28.5	25.8	23.9	242.3	331.1	263.9	1128.3	907.7	1115.1
Lerwick	United Kingdom	1.02	16.4	23.7	14.1	435.7	638.2	478.1	1854.6	1676.1	2004.9
Faraday	United Kingdom	1.19	1.9	2.2	1.9	14.8	31.1	31.8	651.4	2750.4	1911.1
Gibraltar-A	United Kingdom	0.53	120.6	232.6	324.4	2794.6	4331.9	5662.7	7098.9	9844.4	10356.0
Bermuda-B	United Kingdom	0.66	166.7	246.8	297.4	5671.4	7346.2	8175.0	11072.4	12856.3	12385.2
Newlyn, Cornwall	United Kingdom	1.34	73.3	73.0	71.5	595.9	882.0	773.3	2407.4	2904.6	3193.0
Seward-C, AK	USA	1.54	0.6	0.8	0.7	46.5	55.5	52.7	336.0	392.6	396.4
Ketchikan, AK	USA	1.70	4.7	5.1	5.8	123.7	142.7	162.8	677.6	705.6	860.0
Valdez, AK	USA	1.51	0.3	0.5	0.3	36.0	42.8	39.6	256.3	311.5	293.8
Yakutat, AK	USA	1.37	0.0	0.0	0.0	22.0	25.0	25.1	142.8	132.8	148.4
Seldovia, AK	USA	2.09	0.1	0.1	0.1	2.6	2.7	2.8	72.2	73.9	71.3
Sitka, AK	USA	1.42	1.2	1.2	1.5	89.1	102.7	114.4	527.2	520.7	640.7

Continued on next page

Table S-5 – continued from previous page

			100-yr Extreme Sea Level Event								
			2050			2100			2150		
Site	Region	Historical Height (m above MHHW)	AF 1.5°C	AF 2.0°C	AF 2.5°C	AF 1.5°C	AF 2.0°C	AF 2.5°C	AF 1.5°C	AF 2.0°C	AF 2.5°C
Sand Point, AK	USA	1.28	13.2	14.7	17.1	456.0	534.1	693.4	2381.1	2738.8	3388.3
Dutch Harbor-B, AK	USA	0.79	3.0	3.3	4.8	325.9	396.9	499.9	1216.5	1446.2	1703.7
Cordova-B, AK	USA	1.64	8.1	11.0	10.1	315.2	410.8	415.6	2168.9	2366.3	2714.6
Kodiak Isl., AK	USA	1.52	0.3	0.3	0.3	10.3	11.5	11.7	120.8	115.8	121.7
Adak, AK	USA	0.96	6.6	8.4	9.5	465.5	625.5	765.6	1894.5	2248.0	2657.3
San Francisco, CA	USA	0.89	20.9	37.4	43.0	1862.6	2897.6	3773.2	7218.9	10012.1	9777.9
San Diego, CA	USA	0.77	251.4	383.7	411.3	4664.5	6876.2	7692.4	10976.8	13033.2	13177.6
Los Angeles, CA	USA	0.72	169.6	289.9	306.7	3147.8	4902.9	5711.6	8148.9	10843.2	10735.5
Crescent City, CA	USA	1.10	4.7	6.9	8.5	333.2	407.6	613.5	1683.9	2724.7	2370.6
Monterey, CA	USA	0.81	49.9	90.2	107.1	2367.2	3692.7	4598.4	7543.1	10290.9	10081.9
Port San Luis, CA	USA	0.82	35.4	68.9	80.5	1728.2	2692.8	3477.8	5959.1	8809.4	8470.2
Santa Monica, CA	USA	0.84	55.4	111.1	118.2	2235.5	3513.2	4258.3	7213.7	9992.2	9782.9
La Jolla, CA	USA	0.72	329.9	497.5	533.7	5613.6	8042.7	8838.9	11783.7	13605.5	13816.1
New London, CT	USA	1.68	2.9	3.2	3.5	160.3	278.1	286.7	1045.8	2649.5	1753.3
Fernandina Beach, FL	USA	1.20	13.5	15.1	19.5	678.5	1427.8	1514.7	4052.6	7142.1	6672.3
St. Petersburg, FL	USA	1.54	2.1	2.3	2.3	192.5	355.9	340.8	1786.0	3757.1	2908.5
Pensacola, FL	USA	2.23	1.3	1.3	1.4	32.2	47.2	45.6	362.3	729.3	473.0
Mayport, FL	USA	0.79	95.2	119.5	173.4	3432.2	6534.1	7110.6	9685.7	12408.2	13272.1
Limetree Bay, FL	USA	0.87	2.1	2.6	3.3	1453.8	2726.7	2723.5	6852.0	9758.5	9893.3
Key West, FL	USA	0.66	104.2	196.5	224.2	6695.1	9490.6	11079.6	12454.2	14341.5	14984.0
Fort Pulaski, GA	USA	0.98	57.3	65.2	101.7	2378.9	4714.4	5167.3	8784.2	11773.6	12517.1
Hilo, HI	USA	0.55	1019.3	1348.5	1770.1	13959.2	15198.7	15730.0	16186.0	16962.9	16870.4
French Frigate, HI	USA	0.44	1601.0	2844.3	2843.9	13235.9	15124.0	15675.0	14923.7	16242.3	16181.3
Kahului, HI	USA	0.45	2230.5	2844.9	3515.4	14996.6	15859.7	16365.4	16254.4	17011.7	16929.6
Mokuoloe, HI	USA	0.41	2370.9	3099.5	3748.0	14542.8	15533.4	16062.1	15649.4	16717.8	16628.3
Honolulu-B, HI	USA	0.41	2321.5	3047.9	3684.1	14522.1	15519.4	16051.8	15639.2	16710.6	16622.9
Nawiliwili, HI	USA	0.53	412.1	581.2	726.9	10087.8	12243.4	12778.9	13366.7	15278.3	15185.0
Grand Isle, LA	USA	3.72	1.3	1.4	1.3	2.0	2.5	2.2	203.0	341.6	244.7
Woods Hole, MA	USA	1.31	8.1	10.4	11.9	525.5	1271.2	1159.5	2716.7	6231.8	5010.6
Nantucket, MA	USA	2.02	1.7	1.8	1.8	75.8	133.8	141.3	654.8	1512.0	942.2
Boston, MA	USA	1.41	9.4	11.9	13.9	446.5	949.6	966.1	2230.5	5117.3	3864.4
Portland, ME	USA	1.16	26.6	38.3	43.4	768.6	1740.5	1708.6	2861.0	6293.8	5127.9
Eastport, ME	USA	1.51	26.1	39.6	45.4	473.5	1065.4	1027.4	1831.6	4352.6	2978.1
Duck Pier, NC	USA	1.17	26.1	39.8	50.1	1321.7	3181.0	3402.5	6730.1	10270.2	10648.7
Wilmington, NC	USA	0.90	11.9	57.6	40.9	1530.6	3704.6	4085.1	6832.4	10348.1	10725.5
Atlantic City, NJ	USA	1.30	14.4	20.5	25.3	922.4	2332.3	2326.0	4988.2	9017.5	8878.6
Cape May, NJ	USA	1.18	22.9	29.3	38.8	1158.9	3215.4	3098.3	5988.6	9903.3	10461.6
Montauk, NY	USA	1.27	13.0	16.6	19.6	665.5	1506.9	1511.5	3398.0	7236.6	6569.6
New York, NY	USA	1.80	2.6	2.8	3.1	138.1	245.3	254.9	975.7	2462.9	1579.0
Charleston, OR	USA	1.09	20.9	27.1	33.4	721.4	935.4	1392.4	3393.5	5374.5	4857.0
South Beach, OR	USA	1.23	18.7	23.9	28.2	706.6	894.7	1307.8	3659.1	5747.8	5190.7
Astoria, OR	USA	1.16	6.3	8.9	10.9	327.4	400.3	573.2	1611.6	2635.9	2247.8
Newport, RI	USA	1.18	14.2	20.4	23.5	852.3	2073.3	1998.9	3832.3	7736.7	7087.4
Charleston, SC	USA	1.16	8.1	10.7	13.3	874.7	1834.6	2105.4	5292.3	8645.6	8544.7
Galveston (Pier 21), TX	USA	1.86	2.9	3.1	3.1	213.0	425.1	408.2	3085.0	6122.0	5150.0
Rockport, TX	USA	1.19	5.4	9.7	7.0	1643.9	3919.2	4227.0	10407.0	13106.6	13498.7

Continued on next page

Table S-5 – continued from previous page

			100-yr Extreme Sea Level Event								
			2050			2100			2150		
Site	Region	Historical Height (m above MHHW)	AF 1.5°C	AF 2.0°C	AF 2.5°C	AF 1.5°C	AF 2.0°C	AF 2.5°C	AF 1.5°C	AF 2.0°C	AF 2.5°C
Port Isabel, TX	USA	1.36	2.2	2.4	2.5	364.4	850.2	860.0	3656.4	6817.8	5831.2
Galveston (P. Pier), TX	USA	2.61	1.7	1.7	1.8	38.2	61.0	60.5	650.8	1302.6	882.7
Chesapeake BBT, VA	USA	1.53	6.6	7.7	9.2	383.8	892.1	938.6	3049.8	6336.0	5463.1
Neah Bay, WA	USA	1.24	2.5	3.9	5.2	169.5	202.2	275.0	826.5	1252.0	1060.8
Willapa Bay, WA	USA	1.74	2.8	3.3	3.6	109.0	122.9	181.4	777.0	1175.1	998.0
Lewes, DE	USA	1.58	4.4	4.9	5.8	266.4	676.8	641.7	2044.9	4866.3	3667.6
Apra Harbor, Guam	USA Trust	0.40	2138.7	2913.5	3309.0	13694.8	14973.5	16355.9	15592.5	16322.1	16889.6
Wake	USA Trust	1.01	4.8	16.2	7.2	1836.7	3238.3	3214.6	6590.6	9596.9	9391.7
Johnston	USA Trust	0.74	73.1	125.2	103.5	4579.9	7269.6	7508.4	9652.3	12268.5	12261.0
Midway	USA Trust	0.88	13.5	49.3	52.0	2248.3	3983.8	5078.1	7724.6	10549.7	10405.4
Pago Pago	USA Trust	0.45	2238.0	3540.5	3610.3	15988.9	16896.3	17068.8	17038.9	17492.6	17504.5
Charlotte Amalie, VI	USA Trust	0.64	56.7	77.8	85.6	4971.8	7532.7	8019.8	10961.6	13091.4	13770.7
San Juan, PR	USA Trust	0.57	168.6	213.9	264.3	7732.1	10100.8	11083.4	12734.5	14469.1	15217.9
Magueyes Island, PR	USA Trust	0.56	116.6	166.7	188.9	7131.8	9573.7	10447.2	12190.8	14102.5	14788.7

Table S-6: Expected extreme sea level event amplification factors (AF) for the 500-yr event for 2050, 2100, and 2150 under 1.5°C, 2.0°C, and 2.5°C global mean surface temperature stabilization scenarios.

			500-yr Extreme Sea Level Event								
			2050			2100			2150		
Site	Region	Historical Height (m above MHHW)	AF 1.5°C	AF 2.0°C	AF 2.5°C	AF 1.5°C	AF 2.0°C	AF 2.5°C	AF 1.5°C	AF 2.0°C	AF 2.5°C
Buenos Aires	Argentina	4.06	1.3	1.4	1.4	2.1	2.6	2.6	55.2	176.9	103.6
Fort Denison	Australia	0.81	140.1	417.0	328.0	8886.4	17256.4	19629.2	31008.8	50760.8	50147.7
Bundaberg	Australia	1.60	2.8	3.7	3.4	684.9	1062.0	1256.4	6766.1	13232.7	11114.3
Brisbane	Australia	0.89	106.8	265.3	204.7	8695.4	16746.7	17472.4	31697.3	50574.0	47257.0
Spring Bay	Australia	0.84	61.3	177.8	244.7	8283.2	19747.8	19468.0	34215.5	53340.6	51023.0
Townsville	Australia	1.49	33.8	62.7	51.9	1663.0	2675.6	3255.1	11401.2	20902.4	18323.5
Broome	Australia	2.50	86.6	110.5	126.0	1009.6	1412.3	1600.0	4254.6	6664.0	5805.8
Cocos	Australia	0.65	1992.9	2610.7	4122.7	44672.6	58532.5	63192.4	70400.1	77491.9	79104.8
Darwin	Australia	1.83	41.0	60.7	71.0	1633.5	2428.7	2781.0	8700.4	14449.1	12567.6
Esperance	Australia	0.86	378.0	502.8	667.0	12828.6	20452.6	24773.6	40667.0	56465.2	55478.8
Fremantle	Australia	1.00	60.8	96.4	141.5	6487.6	11440.6	13827.7	30536.7	47834.8	45441.2
Cananeia	Brazil	1.79	3.5	4.2	4.0	488.0	1045.8	1015.1	8244.2	17967.7	13235.0
Ilha Fiscal, RJ	Brazil	1.25	12.3	20.3	17.6	2212.9	5027.7	4592.0	17895.9	32603.8	27945.6
Victoria, BC	Canada	1.14	19.6	28.5	38.1	2017.6	2523.6	3540.8	10445.8	17023.5	14649.5
Prince Rupert	Canada	1.84	18.3	20.6	22.6	730.8	852.2	969.3	4353.1	4637.2	5566.3
Tofino	Canada	1.39	3.7	5.3	7.5	652.9	760.7	1028.7	3714.7	5400.1	4680.8
St. John's-A	Canada	1.19	31.2	61.7	69.0	2907.2	7554.2	7388.3	12158.8	30028.5	20758.5
Halifax	Canada	1.45	9.7	13.6	15.7	1812.6	4720.3	4020.0	10383.4	26220.8	17591.6
Churchill	Canada	1.94	0.2	0.3	0.3	2.0	16.1	7.9	253.0	253.2	248.2
Puerto Montt	Chile	1.76	46.7	68.8	81.5	782.7	1260.4	1405.5	4380.3	8032.8	6468.1
Juan Fernandez-B	Chile	0.69	120.2	222.8	269.1	11799.0	19649.3	23222.1	37120.8	51922.7	49780.7
Antofagasta	Chile	0.71	21.7	64.0	79.8	5994.1	11980.6	13259.2	24743.2	40844.8	37972.0
Easter-C	Chile	1.29	2.3	2.6	2.5	983.6	1538.0	1734.4	10741.9	18340.6	17686.1
Valparaiso	Chile	0.66	71.2	170.5	182.3	6152.9	12745.6	13942.4	23933.8	39889.5	36961.1
Xiamen	China	1.93	8.4	10.9	13.9	600.9	765.2	1133.6	5211.1	9256.5	8344.8
Buenaventura	Colombia	1.30	82.5	154.4	149.4	3715.0	6061.5	6622.4	18562.8	31468.7	27534.1
Tumaco	Colombia	1.11	22.7	52.2	52.6	2288.2	3895.6	4291.0	11635.4	21312.0	17863.7
Cartagena	Colombia	0.34	77604.5	70595.5	78784.1	91089.3	90310.5	91263.7	90921.9	90080.9	91141.8
Penrhyn	Cook Islands	0.76	43.8	170.7	112.3	18501.9	27649.0	31501.4	49404.5	62325.7	62025.8
Quepos-A	Costa Rica	0.81	968.4	1329.3	1413.4	18470.1	28720.8	31933.3	46845.8	60621.9	59788.7
Hornbaek	Denmark	1.65	12.4	679.5	10.3	527.3	7339.0	622.7	3732.0	11066.8	3650.3
Gedser	Denmark	2.02	4.1	101.3	3.7	239.9	2508.6	276.2	2286.8	5070.5	2200.4
Baltra-B	Ecuador	0.87	182.5	310.9	330.8	11285.9	18407.4	20817.1	36628.9	51763.7	50080.0
Santa Cruz	Ecuador	0.73	599.0	1038.2	1073.5	21497.4	32044.0	35768.2	48346.4	61527.5	61057.1
La Libertad	Ecuador	0.92	455.4	735.7	751.0	22829.4	34204.8	37733.2	59556.4	70234.9	70766.3
Acajutla-A	El Salvador	0.77	633.2	1013.0	1117.3	22871.5	34292.6	37700.7	53616.8	65245.1	65437.1
Chuuk	Fd. St. Micronesia	1.00	3.0	5.8	4.6	4589.7	10514.5	10318.9	25427.2	39131.3	36683.8
Kapingamarangi	Fd. St. Micronesia	0.67	782.5	1094.9	1303.4	33504.0	45643.4	49964.1	60076.9	70478.2	70982.7
Pohnpei-B	Fd. St. Micronesia	0.73	506.2	739.1	677.8	24526.3	39212.7	42594.9	54366.3	65977.2	66246.9
Yap-B	Fd. St. Micronesia	2.66	1.2	1.2	1.2	104.4	123.0	142.5	1304.5	2090.9	1670.7
Suva-C	Fiji	0.72	1159.3	1525.4	1526.3	49072.7	53962.0	64401.7	75006.9	80670.8	78583.7
Noumea	France	0.54	2746.4	4059.8	3758.3	44700.2	57259.2	64775.0	64193.9	75817.2	73139.2

Continued on next page

Table S-6 – continued from previous page

			500-yr Extreme Sea Level Event								
			2050			2100			2150		
Site	Region	Historical Height (m above MHHW)	AF 1.5°C	AF 2.0°C	AF 2.5°C	AF 1.5°C	AF 2.0°C	AF 2.5°C	AF 1.5°C	AF 2.0°C	AF 2.5°C
Brest	France	1.87	115.9	97.9	136.0	1026.2	1434.3	1611.9	4835.9	7253.0	5784.4
Marseille	France	0.98	22.8	1498.4	32.5	2879.2	16891.3	4212.0	18005.9	31558.7	25658.5
Rikitea	French Polynesia	0.34	17923.6	28527.1	27327.6	75623.9	81159.5	82681.6	80287.1	84612.2	83200.8
Papeete-B	French Polynesia	0.93	3.1	4.3	4.5	8016.7	14099.5	14806.4	37757.6	53629.0	49952.3
Cuxhaven	Germany	4.10	2.0	2.1	1.9	5.6	13.5	6.5	271.2	221.4	219.8
Malin Head	Ireland	1.68	6.8	9.6	4.9	441.7	813.8	429.7	3056.8	2509.0	2837.7
Hakodate	Japan	0.61	326.2	578.1	1440.0	13620.2	21590.2	27783.5	34046.9	48511.9	47417.6
Hamada	Japan	1.29	2.9	3.5	5.2	1777.5	2616.0	3940.3	12931.6	23337.7	22407.0
Maisaka	Japan	2.46	1.1	1.1	1.2	3.4	9.5	104.8	700.4	1051.3	1012.8
Ishigaki	Japan	1.09	58.8	86.9	163.9	8460.1	12150.6	16501.6	32864.3	47479.9	46169.3
Naha	Japan	1.17	13.9	23.4	65.3	5069.3	7912.7	11757.7	25559.1	39937.9	38558.7
Toyama	Japan	0.75	195.2	435.0	1203.7	24147.3	36097.7	41566.8	53178.6	66918.1	64621.7
Hosojima	Japan	1.55	2.1	2.4	2.9	600.1	754.8	1213.5	5079.2	9439.6	8894.4
Kushiro	Japan	0.79	7610.9	13840.2	17024.8	90530.4	88963.4	90649.1	91263.4	90603.5	91252.7
Abashiri	Japan	0.85	170.7	495.9	642.5	12971.3	21594.0	25458.6	40924.5	53743.9	52938.6
Mera	Japan	1.20	9.6	11.7	29.1	7307.3	13047.2	15680.7	39584.4	55059.4	54061.1
Wakkanai	Japan	0.99	16.0	40.6	140.5	9767.9	14726.5	20351.0	40071.8	54357.7	53130.1
Chichijima	Japan	1.19	5.5	16.1	29.0	7254.1	9933.8	13937.8	30201.2	43733.7	42721.9
Nishinoomote	Japan	1.04	47.8	77.4	207.8	8348.8	13568.1	17387.5	32883.3	48620.1	47383.7
Naze	Japan	1.28	11.6	14.9	39.1	4883.2	7607.8	10461.1	25581.5	40977.5	39627.9
Hachinohe	Japan	0.82	481.0	672.3	1676.0	38845.4	52194.5	56024.8	71518.0	78998.5	78055.4
Miyakejima	Japan	1.68	9.0	9.7	15.6	5877.6	8593.5	10967.2	43137.1	57874.4	57819.2
Nakano Shima	Japan	1.57	2.7	2.9	4.0	1580.9	2132.4	2975.9	12922.1	22752.9	21890.3
Ofunato	Japan	0.74	5729.3	8444.9	14293.2	86028.4	88256.2	86997.9	91131.0	90785.6	90446.4
Nagasaki	Japan	1.06	136.5	212.3	345.8	7594.4	11993.6	14921.5	27940.9	42991.6	41186.1
Aburatsu	Japan	1.53	3.2	3.7	4.9	956.9	1332.4	1959.1	8390.2	15334.0	14529.9
Kushimoto	Japan	0.91	409.4	578.8	1087.7	28644.9	41479.1	45581.3	64002.7	74398.6	73182.7
Cendering	Malaysia	1.28	14.6	20.5	25.5	2408.4	4138.2	5049.9	15175.8	25023.1	22419.9
Johor Baharu	Malaysia	1.00	271.2	370.6	432.8	10140.4	15834.9	18920.4	33057.5	46110.6	44257.0
Kuantan	Malaysia	1.28	38.7	54.2	65.3	3441.6	5722.3	7001.2	18965.2	30024.0	27266.0
Keling	Malaysia	0.80	403.5	550.3	652.2	14210.8	20924.7	25283.3	36583.0	48898.9	47111.0
Lumut	Malaysia	0.89	374.8	530.7	643.6	12192.1	18491.5	21731.3	34031.0	47000.2	44571.9
Kelang	Malaysia	1.39	147.2	184.2	213.8	3110.5	4505.1	5516.1	15460.7	23423.4	20903.0
Langkawi	Malaysia	0.97	391.3	563.4	683.6	9368.7	14737.0	17147.5	29150.9	42035.0	39183.9
Penang	Malaysia	0.94	231.2	369.1	482.5	11382.5	17532.5	20569.2	33828.1	46762.9	44395.8
Port Louis-C	Mauritius	0.49	1861.5	3337.8	5555.3	39822.8	55907.3	58428.6	60139.2	72660.3	72840.6
Rodrigues	Mauritius	1.44	2.7	3.1	3.5	1563.5	2230.7	2627.0	12817.9	22700.2	20358.2
Manzanillo-A	Mexico	0.72	1147.4	1952.5	2007.0	56380.3	65292.1	69484.6	80779.5	82764.3	84203.4
Ensenada	Mexico	0.73	1279.6	1984.0	2097.3	24912.4	36287.0	40461.7	55045.1	65169.5	65936.1
Salina Cruz	Mexico	0.89	53.4	107.0	129.4	14646.9	25030.4	27551.9	49463.4	62329.3	62130.5
Acapulco-A, Gro.	Mexico	0.89	155.7	305.0	320.9	42263.4	53990.4	58341.7	79199.2	81918.6	83379.7
Cabo San Lucas	Mexico	0.64	1493.7	2284.2	2320.8	30040.5	42154.2	45808.9	56647.4	66784.1	67317.6
Guaymas	Mexico	0.72	818.6	1381.1	1888.2	46485.5	57032.5	60584.8	76118.4	80319.1	81660.3
Saipan-B	N. Mariana Islands	3.88	1.1	1.1	1.1	1.2	1.3	1.3	256.9	332.7	296.6
Marsden Point	New Zealand	5.34	1.1	1.1	1.1	1.2	1.2	1.2	1.5	9.8	1.6
Tauranga	New Zealand	0.63	670.2	2658.2	1980.1	27902.4	48652.1	51463.7	53690.5	72957.9	71921.3

Continued on next page

Table S-6 – continued from previous page

			500-yr Extreme Sea Level Event								
			2050			2100			2150		
Site	Region	Historical Height (m above MHHW)	AF 1.5°C	AF 2.0°C	AF 2.5°C	AF 1.5°C	AF 2.0°C	AF 2.5°C	AF 1.5°C	AF 2.0°C	AF 2.5°C
Taranaki	New Zealand	4.03	1.1	1.2	1.2	1.4	1.5	1.5	168.2	192.4	160.8
Wellington	New Zealand	0.65	879.9	3421.7	2399.5	35806.3	57085.7	59749.9	62613.0	79421.6	79116.0
Tregde	Norway	1.18	9.1	25.7	8.1	1157.6	2301.0	1369.7	6583.6	6521.2	6963.8
Rorvik	Norway	2.41	1.1	1.1	1.1	11.0	121.6	19.5	593.9	528.0	530.7
Ny-Alesund	Norway	0.83	1.9	586.5	0.1	188.7	675.7	167.7	2056.9	796.6	1239.7
Vardo	Norway	1.37	6.5	88.3	14.8	562.3	1857.7	1024.7	3123.2	4974.1	4103.3
Balboa	Panama	1.38	266.5	341.8	363.7	3224.8	5313.5	5644.4	15314.4	26744.1	23949.3
Cristobal	Panama	0.40	9401.0	14165.8	16579.4	66373.5	76607.5	83001.3	74870.4	82498.4	84285.2
Rabaul	Papua New Guinea	0.38	11126.5	15096.6	17205.6	65745.6	72307.3	78677.4	75052.7	81087.2	82152.9
Lobos de Afuera	Peru	0.72	283.7	598.3	596.2	17958.0	28032.1	30937.5	43680.5	57622.7	56660.0
Callao-B	Peru	0.80	9.4	22.0	33.9	5925.6	10511.0	11551.3	25256.4	40364.0	37832.2
Legaspi	Philippines	0.77	673.1	1343.4	1393.0	40173.8	54681.0	61471.9	71715.1	78353.8	80502.8
Manila	Philippines	0.99	1332.3	1966.0	2170.0	70657.2	78518.8	83131.0	90542.3	89503.4	90784.7
Cascais	Portugal	1.11	157.1	132.6	234.0	3481.6	5522.9	7401.8	17524.5	27515.4	26167.1
Funchal-B	Portugal	0.71	2595.5	2369.3	3691.3	27985.3	37824.0	43838.4	53382.1	63598.9	68858.4
Kanton-B	Rep. of Kiribati	0.66	305.4	493.3	530.6	24581.8	36371.1	37964.7	51936.2	63779.0	64339.6
Christmas-B	Rep. of Kiribati	0.52	2659.3	4775.0	4584.9	55856.8	63567.3	66281.2	71002.7	77636.9	78907.4
Majuro-A	Rep. of Marshall I	0.65	3520.2	4557.4	4319.1	44197.7	55526.8	60562.8	67226.0	75519.9	76976.1
Kwajalein	Rep. of Marshall I	0.56	6919.4	8953.7	8653.8	57312.2	68330.6	72563.4	74185.6	79518.4	81949.8
Malakal-B	Republic of Belau	0.56	4055.8	5354.7	5800.7	46906.4	64135.1	67405.4	69621.6	77950.4	78802.5
Kaohsiung	Republic of China	1.07	3.7	5.7	7.7	2919.6	4617.4	6051.7	15200.5	25186.0	23263.8
Keelung	Republic of China	1.45	3.2	3.7	4.4	1642.1	2547.8	3234.1	13595.5	22877.9	21736.3
Luderitz	South Africa	0.64	1659.4	2153.5	2520.5	35516.9	49347.3	55117.9	60534.1	72222.6	74333.9
Saldahna Bay	South Africa	0.63	3032.7	3659.9	4283.5	37526.0	51160.7	55194.0	60240.2	71743.0	73096.6
Simon's Town	South Africa	0.80	510.5	696.2	876.7	21247.5	33659.0	38075.0	52483.8	66983.0	67917.7
Port Nolloth	South Africa	0.72	1340.0	1690.2	1782.6	26866.5	40205.9	44635.6	55028.3	68540.1	70131.1
Port Elizabeth	South Africa	0.95	169.6	268.9	281.2	8439.8	14608.6	17137.7	31546.8	48595.9	46833.7
La Coruna	Spain	1.22	364.3	305.9	417.6	4283.3	6170.7	7502.6	19546.4	27540.6	26957.9
Ceuta	Spain	0.60	313.2	745.4	1012.2	13028.3	20613.8	26894.6	37665.3	51148.2	53923.1
Vigo	Spain	1.64	7.4	6.8	9.6	848.1	1300.8	1615.9	7265.2	10869.4	9449.6
Stockholm	Sweden	1.14	3.0	6322.5	1.7	527.1	16474.3	546.0	1935.5	378.9	2299.0
Goteborg-Torsh.	Sweden	1.69	2.7	45.7	2.3	270.2	2228.4	293.3	2088.2	3290.9	1939.3
Zanzibar	Tanzania	1.13	968.3	1163.0	1239.8	7836.2	11838.3	14099.2	25322.7	39533.9	37720.3
Ko Lak	Thailand	1.13	280.1	372.3	416.4	9471.4	15073.0	17685.9	34715.6	47820.4	45893.2
Stornoway	United Kingdom	1.56	80.1	72.0	63.1	985.9	1364.4	1054.2	4992.6	3963.7	4853.8
Lerwick	United Kingdom	1.17	16.7	28.7	14.1	1320.5	1881.5	1401.7	6700.6	5780.6	6820.8
Faraday	United Kingdom	1.77	1.3	1.4	1.3	1.8	2.3	2.4	345.5	2886.0	1308.8
Gibraltar-A	United Kingdom	0.63	107.1	412.2	556.2	7756.5	13043.1	17040.4	26715.8	40410.3	41853.7
Bermuda-B	United Kingdom	0.79	170.3	352.3	375.8	15346.2	21977.7	25851.6	44163.7	54173.8	50627.4
Newlyn, Cornwall	United Kingdom	1.39	232.5	231.0	224.6	2458.7	3688.1	3198.8	10690.8	12806.8	14037.9
Seward-C, AK	USA	1.77	0.6	0.8	0.7	149.4	172.0	163.9	1227.9	1446.5	1401.0
Ketchikan, AK	USA	1.81	6.3	6.6	8.0	433.4	498.6	558.3	2721.4	2809.8	3417.9
Valdez, AK	USA	1.69	0.3	0.5	0.4	114.7	133.9	116.4	1019.5	1227.7	1152.2
Yakutat, AK	USA	1.41	0.0	0.0	0.1	89.3	101.3	102.0	684.8	633.9	701.0
Seldovia, AK	USA	2.36	0.2	0.2	0.2	4.8	5.1	5.1	274.3	286.3	270.9
Sitka, AK	USA	1.55	1.4	1.4	1.7	316.4	358.5	389.5	2087.7	2057.6	2512.7

Continued on next page

Table S-6 – continued from previous page

			500-yr Extreme Sea Level Event								
			2050			2100			2150		
Site	Region	Historical Height (m above MHHW)	AF 1.5°C	AF 2.0°C	AF 2.5°C	AF 1.5°C	AF 2.0°C	AF 2.5°C	AF 1.5°C	AF 2.0°C	AF 2.5°C
Sand Point, AK	USA	1.37	25.1	28.2	34.3	1646.3	1939.9	2498.4	9683.5	11038.9	13710.8
Dutch Harbor-B, AK	USA	0.83	8.2	8.5	13.2	1417.3	1747.1	2174.4	5565.5	6606.8	7766.8
Cordova-B, AK	USA	1.92	4.7	6.2	5.7	588.9	749.2	747.5	5809.9	6310.5	7127.9
Kodiak Isl., AK	USA	2.08	0.5	0.5	0.5	1.9	2.1	2.1	316.9	288.6	290.6
Adak, AK	USA	1.11	5.9	8.0	8.8	1435.4	1862.4	2192.5	6720.6	7913.4	9312.7
San Francisco, CA	USA	1.06	15.6	28.2	32.6	4198.8	6260.8	8878.8	23348.1	37041.7	34460.2
San Diego, CA	USA	0.82	692.8	1176.1	1272.6	18432.8	28003.3	32076.3	49790.4	61417.2	61774.5
Los Angeles, CA	USA	0.76	504.7	959.2	1013.6	12969.8	20389.1	24300.6	37088.4	51059.3	50167.2
Crescent City, CA	USA	1.20	7.5	11.4	14.6	1190.2	1428.3	2118.3	6669.7	10753.7	9311.0
Monterey, CA	USA	0.90	77.7	156.9	189.6	7628.1	11976.3	15660.7	30373.1	44468.8	42680.2
Port San Luis, CA	USA	0.91	52.4	117.2	138.8	5682.4	8701.1	11797.1	23658.5	37449.5	35070.6
Santa Monica, CA	USA	0.96	52.4	131.8	139.1	6351.2	9990.3	12777.2	26826.7	40936.5	38899.2
La Jolla, CA	USA	0.76	1093.3	1738.8	1872.2	23299.6	34565.4	38633.5	54876.0	65149.7	65888.9
New London, CT	USA	2.32	2.1	2.2	2.4	182.6	239.3	280.6	1627.1	3602.0	2298.1
Fernandina Beach, FL	USA	1.47	7.3	8.2	10.4	1238.0	2386.6	2499.9	10169.9	20097.6	16345.2
St. Petersburg, FL	USA	2.61	1.5	1.5	1.5	107.3	152.7	147.5	1326.4	2288.1	1683.6
Pensacola, FL	USA	4.96	1.1	1.1	1.1	1.3	1.3	1.3	118.0	160.9	120.4
Mayport, FL	USA	0.95	58.9	79.1	125.7	7495.2	16304.5	17497.2	33566.1	50012.6	51589.2
Limetree Bay, FL	USA	2.44	1.2	1.2	1.2	103.3	140.4	141.6	1451.3	2102.9	1789.8
Key West, FL	USA	0.96	8.3	18.9	20.6	6885.1	14446.8	15694.8	33993.6	50454.3	50608.7
Fort Pulaski, GA	USA	1.17	34.4	40.9	65.8	4810.2	10236.3	11249.8	27865.7	44532.3	44427.6
Hilo, HI	USA	0.67	1101.5	1397.8	2064.4	50208.0	60633.9	64769.0	72650.8	79834.2	79266.5
French Frigate, HI	USA	0.47	5166.8	9932.6	9631.2	61693.1	72363.0	75201.3	72575.1	79889.3	79566.0
Kahului, HI	USA	0.52	4358.4	5762.7	7470.3	64469.3	71870.2	75026.6	76638.6	82479.4	81936.2
Mokuoloe, HI	USA	0.44	7985.3	10686.6	13081.3	68242.5	74590.5	77354.4	76141.2	82417.7	81903.1
Honolulu-B, HI	USA	0.45	6765.5	9160.8	11269.1	66497.3	73348.5	76208.8	75332.6	81936.3	81406.4
Nawiliwili, HI	USA	0.70	255.7	311.7	433.1	25034.2	36740.1	39467.1	52436.1	65202.0	64481.3
Grand Isle, LA	USA	10.00	1.3	1.3	1.3	1.4	1.4	1.4	1.6	1.7	1.6
Woods Hole, MA	USA	1.64	5.6	6.7	7.6	944.6	1845.4	1741.2	6121.0	15575.5	9985.3
Nantucket, MA	USA	3.73	1.3	1.3	1.3	1.7	2.0	2.1	371.7	610.4	413.6
Boston, MA	USA	1.75	5.1	6.1	7.1	791.8	1415.8	1443.9	5092.7	12216.2	7840.9
Portland, ME	USA	1.33	26.9	41.6	45.4	2017.1	4466.7	4331.1	9306.0	22440.0	15797.1
Eastport, ME	USA	1.72	19.6	33.1	35.1	1154.5	2613.2	2474.6	5692.4	14255.0	8828.9
Duck Pier, NC	USA	1.39	19.4	30.8	38.9	2593.4	6307.6	6914.5	18914.9	36160.4	32678.8
Wilmington, NC	USA	1.23	4.2	7.6	6.3	1856.4	4229.3	4712.1	13864.5	28659.9	23977.8
Atlantic City, NJ	USA	1.61	8.6	11.2	13.5	1447.1	3423.2	3402.7	10893.4	25955.7	19516.2
Cape May, NJ	USA	1.44	13.7	17.3	22.7	2037.3	5620.2	5274.3	14634.9	32519.3	27706.1
Montauk, NY	USA	1.53	10.7	13.5	16.1	1334.7	2747.3	2727.3	8669.7	21675.4	15659.8
New York, NY	USA	2.61	1.8	1.8	2.0	129.2	169.7	191.8	1256.3	2536.5	1604.0
Charleston, OR	USA	1.18	38.2	54.1	70.4	2539.1	3202.8	4868.6	13534.4	21855.9	19414.6
South Beach, OR	USA	1.36	24.9	34.4	42.0	2142.7	2630.7	3913.2	13161.3	21263.6	18739.4
Astoria, OR	USA	1.25	10.0	15.6	20.2	1201.0	1428.7	2069.0	6522.4	10608.8	8964.0
Newport, RI	USA	1.46	8.4	11.0	12.9	1531.5	3425.3	3211.7	9214.2	22786.3	16017.0
Charleston, SC	USA	1.60	3.2	3.3	3.8	873.0	1521.8	1745.7	8442.7	16501.4	13318.9
Galveston (Pier 21), TX	USA	2.97	1.8	1.8	1.9	60.0	154.1	150.3	1616.6	3098.3	2045.8
Rockport, TX	USA	1.98	2.1	2.2	2.2	480.3	927.0	937.2	7508.1	15623.2	11228.3

Continued on next page

Table S-6 – continued from previous page

			500-yr Extreme Sea Level Event								
			2050			2100			2150		
Site	Region	Historical Height (m above MHHW)	AF 1.5°C	AF 2.0°C	AF 2.5°C	AF 1.5°C	AF 2.0°C	AF 2.5°C	AF 1.5°C	AF 2.0°C	AF 2.5°C
Port Isabel, TX	USA	2.74	1.3	1.3	1.4	37.8	129.6	134.7	1294.2	2070.5	1554.8
Galveston (P. Pier), TX	USA	5.23	1.3	1.2	1.3	1.6	1.7	1.7	155.8	201.4	162.0
Chesapeake BBT, VA	USA	2.03	3.3	3.7	4.1	421.2	858.5	919.4	4698.6	10481.4	7172.8
Neah Bay, WA	USA	1.31	4.3	7.2	10.8	680.6	803.2	1108.3	3609.0	5333.6	4552.7
Willapa Bay, WA	USA	2.05	2.2	2.5	2.8	245.7	260.9	376.5	2165.3	3143.7	2681.3
Lewes, DE	USA	2.17	2.5	2.6	2.9	264.0	519.5	578.1	2925.3	6571.5	4239.6
Apra Harbor, Guam	USA Trust	0.50	2417.5	3795.5	3740.8	53177.4	64135.3	71182.3	70432.7	77042.4	79708.6
Wake	USA Trust	1.83	1.5	1.6	1.6	579.3	967.9	851.4	5291.3	9615.6	8276.6
Johnston	USA Trust	0.90	55.8	106.3	83.5	10912.5	20817.0	21165.6	35398.3	49761.8	49145.3
Midway	USA Trust	1.11	8.0	16.5	18.8	4050.6	7457.0	9606.3	23615.0	37527.5	35187.7
Pago Pago	USA Trust	0.48	7261.5	12411.4	12500.4	76295.7	82301.2	83284.4	83756.1	86752.3	86680.1
Charlotte Amalie, VI	USA Trust	1.24	1.8	1.7	1.8	1558.9	2873.0	2539.3	13517.6	24124.4	22018.1
San Juan, PR	USA Trust	0.93	4.3	5.8	7.5	6126.9	11776.5	11300.4	31538.1	46306.3	47042.1
Magueyes Island, PR	USA Trust	1.09	1.9	1.9	2.0	2604.2	5133.4	4682.8	18797.1	32726.1	31089.7